Aalborg University

Identification of Randers Water Distribution Network for Optimal Control

Electronic & IT:
Control & Automation

Group:
CA9-938

Student report

November 8, 2017

Second year of MSc study
Electronic and IT
Fredrik Bajers Vej 7
DK-9220 Aalborg East, Denmark
http://www.es.aau.dk

AALBORG UNIVERSITY
STUDENT REPORT

Topic:

Optimal Control for Water Distribution

Project:

P9-project

Project time:

September 2017 - December 2017

Projectgroup:

17gr938

Participants:

Krisztian Mark Balla

Supervisors:

Tom Nørgaard Jensen
Jan Dimon Bendsten
Carsten Skovmose Kallesøe

Synopsis:

The synopsis is going to be written here...

Circulation: x
Number of pages: x
Appendix: x
Completed xx-xx-2017

Preface

The preface is going to be written here... The preface is going to be written here... The preface is going to be written here... The preface is going to be written here... The preface is going to be written here... The preface is going to be written here... The preface is going to be written here... The preface is going to be written here... The preface is going to be written here... The preface is going to be written here... The preface is going to be written here...

Aalborg University, th of December 2017

Krisztian Mark Balla
kballa16@student.aau.dk

Nomenclature

Acronyms

CT	Circuit Theory
D-W	Darcy-Weisbach
EPA	Environmental Protection Agency
FCV	Flow Control Valve
GIS	Geographic Information Systems
GT	Graph Theory
KCL	Kirchhoff's current law
MPC	Model Predictive Control
PRV	Pressure Regulating Valve
OD	Opening Degree
ODE	Ordinary Differential Equation
WSS	Water Supply System
WT	Water Tank

Acronyms - Randers Network

BKV	Bunkedal Vandværk
LZ	Low Zone
HBP	Hobrovej Pumpestation
HNP	Hornbæk Pumpestation
HSP	Hadsundvej Pumpestation
HZ	High Zone
OMV	Oust Mølle Vandværk
T1A	Water tank A in Hobrovej Pumpestation
T1B	Water tank B in Hobrovej Pumpestation
T2	Water tank in Hadsundvej Pumpestation
TBP	Toldbodgade Pumpestation
VSV	Vilstrup Vandværk
ØSV	Østrup Skov Vandværk

Symbols

Symbol	Description	Unit
A_{wt}	Cross sectional area of water tanks	$[m^2]$
a_{h2}, a_{h1}, a_{h0}	Pump constants	$[\cdot]$
c_D	Darcy-Weisbach equation coefficient	$[\frac{s^2}{m}]$
D	Diameter (of pipes or tanks)	$[m]$
d	Flow demand	$[\frac{m^3}{s}]$
$f(q)$	Pressure drop due to pipe resistance	$[Pa]$
h	Pressure drop due to elevation	$[Pa]$
h_l	Water level in tanks	$[m]$
h_p	Pressure head	$[m]$
h_t	Total head	$[m]$
J	Mass inertia of water pipes	$[kgm^2]$
k_v	Valve conductivity function	$[\cdot]$
l	Length (of pipes)	$[m]$
p	Absolute pressure	$[Pa]$
q	Volumetric flow	$[\frac{m^3}{s}]$
Re	Reynolds number	$[\cdot]$
T	Period of time	$[s]$
z	Elevation head	$[m]$
γp	Resistance parameter of pipes	$[\cdot]$
Δp	Differential pressure	$[Pa]$
ϵp	Roughness of pipes	$[m]$
$\mu(q, k_v)$	Pressure drop on valves	$[Pa]$
ω_r	Impeller rotational speed of centrifugal pumps	$[\frac{rad}{s}]$
τ	Elevated reservoir parameter	$[\frac{Pa}{m^3}]$

Constants

Symbol	Description	Unit
$g = 9.83$	Gravitational acceleration	$[\frac{m}{s^2}]$
$\rho = 1000$	Density of water	$[\frac{kg}{m^3}]$
$f_D = ...$	Darcy friction factor	$[\frac{kg}{m^3}]$

Graph theory

Symbol	Description
B	Cycle matrix
$\mathcal{E}$	Set of edges
$\mathcal{E}_\mathcal{T}$	Edges regarding the sub-graph $\mathcal{T}$
$\mathcal{E}_\mathcal{C}$	Edges regarding the sub-graph $\mathcal{C}$
I	Identity matrix
$\mathcal{G}$	Directed and connected graph
H	Incidence matrix
$\mathcal{V}$	Set of vertices
$\bar{\mathcal{V}}$	Vertices regarding non-inlet points
$\hat{\mathcal{V}}$	Vertices regarding inlet points
c	Number of pumping stations
l	Number of elevated reservoirs
m	Number of columns in the incidence matrix
n	Number of rows in the incidence matrix
$\mathcal{T}$	General sub-graph
$\mathcal{T}^*$	Tree in a graph
$\mathcal{T}^*_{span}$	Spanning tree in a graph

Glossary of mathematical notation

Matrices

Diagonal matrices are noted with $diag(\cdot)$, which maps an n-tuple to the corresponding diagonal matrix:

$$diag \,:\, \mathbb{R}^n \to \mathbb{R}^{n\times n},$$

$$diag(a_1,\,\dots,a_n) := \begin{pmatrix} a_1 & & \\ & \ddots & \\ & & a_n \end{pmatrix}.$$

Contents

1. Introduction

Due to the fast-paced technological development all over the world, the demand for industrial growth and energy resources has seen a rapid increase. Along with the industrial growth, the sudden rise in population has made the world realize that this shortage of energy sources is an actual and universally anticipated problem [1]. In order to cope with such shortage issues and to make the rapid development possible and less expensive, the world is moving towards more efficient use of resources and optimization of infrastructure. Therefore, technological development is also moving the focus on green energy, resulting in more and more renewable energy sources added to the grid [2].

Water Supply Systems(WSSs) are among the sectors which make the industrial growth possible. On top of this, WSSs are one of the most vital infrastructures of modern societies in the world. In Denmark typically, such networks are operating by making pumps transport water from reservoirs through the pipe network, to the end-users. In most cases, elevated reservoirs are exploited in these WSSs, such that they can even out the demand differences for the consumers. Although elevated reservoirs are usually an integrated part of these systems, providing drinking water is a highly energy-intensive activity. For instance, in the United States alone, the drinking water and waste water systems are typically the largest energy consumers, accounting for 25 to 40 percent of a municipality's total public expenditure. [3].

Since fresh water is limited, and due to the presence of global changes such as climate change and urbanization, new trends are emerging in the water supply sector. In the past few decades, several research and case study showed that WSSs and other energy distribution networks need to be improved due to the leakages in the system, high cost of maintenance and due to high energy consumption. Companies also realized that by using proper pressure management in their networks, the effect of leakages can be reduced, thereby huge amount of fresh water can be saved [4].

In Denmark recently, the larger water suppliers have been focusing on making the water supply sector more effective through introducing a benchmarking system focusing on the environment, the security of supply and the efficiency based on user demands. Since 1980, these efficiency activities has been an important issue [5]. It has been proved that by utilizing advanced, energy- or cost-optimizing control schemes and utilizing renewable energy sources, such as elevated reservoirs, the life of the existing infrastructure can be extended and money or energy can be saved [1]. Therefore there is a growing demand in industry for developing methods, leading towards more efficient WSSs.

The presented project is executed in collaboration with the company, Verdo A/S. It is in the interest of Verdo A/S to utilize an advanced model-based optimal control scheme on the WSS with several storages in Randers, Denmark. For a large municipality such as Randers, the water distribution network is complex and consists of thousands of elements. Since the control algorithm itself is complex and model-based, the computational effort is also high. Furthermore, the offline optimisation of a large-scale WSS means that any changes to the network may require significant changes in the optimisation method, which leads to high costs of the system maintenance [6]. Therefore typically a model reduction is required in such networks to make the online execution of the control algorithm possible.

The long-term goal of this project is to find a solution for implementing Model Predictive Control(MPC) on the Randers WSS. However, before the implementation of any control scheme would be possible, a proper and identified model is required. Therefore, as the first part of the project, the following problem statement can be formulated:

How can the WSS in Randers be simplified and identified, with storages included in the system, such that the reduced model preserves the original nonlinear behaviour and remains suitable for a plug-and-play commissionable Model Predictive Control scheme.

Part I

System Analysis

2. Description of Water Supply Systems

This chapter gives a general overview of hydraulic systems and an introduction to the WSS in Randers. The basic topology and structures of water supply networks are explained. The components of hydraulic systems are discussed. Furthermore, the different zones, pumping stations and waterworks are introduced and their role is explained in the Randers WSS.

2.1 Hydraulic system overview

WSSs are designed to deliver water to consumers in terms of sufficient pressure and appropriate chemical composition. Distribution systems as such are typically transport water from one geographical place to another. In practice, there are different methods exist to achieve this water transport. One example is the use of natural advantages such as the water stored in mountains, and thereby use the potential energy of the water to provide pressure in the network. Examples for this are countries like Norway where the advantages of the landscape are being exploited [7]. However, in this project the source of the water is considered as groundwater, considering that in Denmark all reservoirs in the network are tapping water from the ground. It worth noting that the quality of groundwater in Denmark is sufficiently good to use it for drinking water supply purposes. After tapping the water, it goes through an aeration process at the waterworks and afterwards the pure water is pumped into the network [8]. In WSSs, pumps and valves are the elements that enable the control and thereby the proper delivery of water to the consumers or to elevated reservoirs, storing water for later use. Such a network is illustrated in the figure below

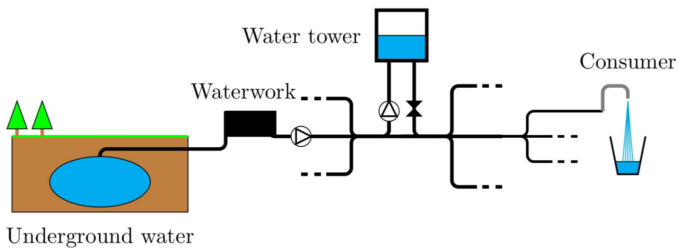

Figure 2.1: Illustration of a WSS [9].

The delivered water needs to fulfil a certain pressure criteria in order to reach consumers at higher levels. For example, in some cases the pressure has to be high enough to make it to the fourth floor of a building and still provide appropriate pressure in the water taps. Generally, in such cases booster pumps are placed in the basement of buildings, helping to supply the pressure. Too large pressure values, however increase water losses due to pipe waste [10].

Another criteria is that the flow through particular pipes need to stay within acceptable limits. A low flow rate can lead to water quality problems due to the undesirable microorganisms in the water and due to the metal and salt accumulation on the wall of the pipes [10].

As can be seen in *Figure 2.1*, typically WSSs consist of pipe, valve, reservoir, elevated reservoir(tank) and pump components. The common property of them is that they are all two-terminal components, therefore they can be characterized by the dynamic relationship between the pressure drop across their two corresponding endpoints and the flow through them [11].

2.1.1 Pipe networks

Pipes have a major role in WSSs since they are used for carrying pressurized water. They serve as a connection between components. Normally, the pipe network can be split into different sub-parts, taking into account the physical characteristics and the attributes of the pipes. Therefore, water supply networks can consist of transmission mains, arterial mains, distribution mains and service lines as shown in the example below:

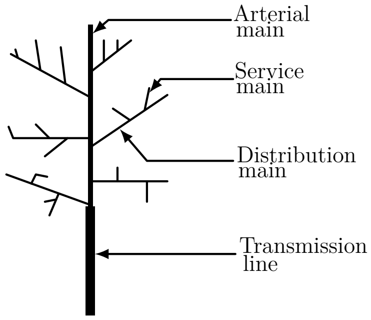

Figure 2.2: Illustration of pipe mains. Tree configuration.

Transmission mains deliver large amounts of water over long distances. Arterial and distribution mains provide intermediate steps towards delivering water to the end-users. Service lines transmit the water from the distribution mains straight to the end-users [12].

The transmission and distribution network can have a topology that is called a loop or a tree structure. *Figure 2.2* shows an example for a tree configuration. This type of configuration is most frequently used in rural areas [13]. Typically the network has only one path for the water to reach the end-users. A more frequent problem compared to looped configurations is, that on the outer parts of the system lower pressures can be experienced due to the pressure losses from long flow paths. The flow dynamics within this kind of systems therefore consist of large flows closer to the source that turn into smaller flows on the outer parts of the system. Main disadvantage of a purely tree structure system is that due to maintenance or momentary breakdowns, the system suffers disruption of service [13].

Loop networks have a configuration as shown in *Figure 2.3*.

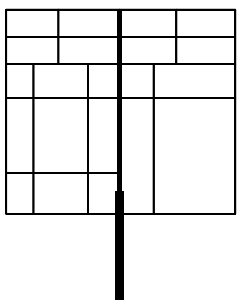

Figure 2.3: Loop configuration.

Loop networks are usually composed of smaller loops which are composed of smaller distribution mains, and larger loops that are connected to arterial or transmission mains. Elevated reservoirs are typically placed in the centre of the system due to pressure losses resulting from flows through the loop network [14]. This is reasonable because within a certain grid, the same pressure is provided by the tank, instead of providing the pressure through long pipelines to different distances. Furthermore, in the presence of a ring structure, the large loop around the area may be used to feed an internal distribution grid or a distribution grid attached to the outer part of the loop. Loop configurations are generally associated with larger suburban and city distribution systems such as larger cities[14]. The Randers WSS falls into this category.

2.1.2 Elevated reservoirs

Elevated reservoirs, or tanks, are typically placed in the system to use them as buffers and level out the pressure and flow demand differences. When the demand is high, the waterworks might not be able to provide the sufficient amount of water in the network. In these cases, the elevated reservoir supplies the remaining demand. When the user consumption decreases, the system can be controlled such that the tank is being refilled to provide the required demand for the next peak time of consumption. Having such an elevated reservoir in the network, the system becomes more independent of the pump stations, as the refilled tank can itself maintain the desired pressure and flow for a limited time.

Due to the elevation of the tank, when it is filled up, the pumping stations need to provide a pressure higher than the pressure in the water tank(WT). Therefore when the tank is being emptied, the pumping stations can reduce the amount of pressure they provide to the system, since the pressure from the elevated reservoir becomes dominant. This is due to the fact that the dynamics of systems with large storages come primarily from the pressure of the tank [15]. However, it should be noted that normally the level in the tank is varying less than a meter. This means that the effect on the pump operation is limited. Due to these considerations, the dynamics of these elevated reservoirs has to be taken into account while modelling the system.

2.1.3 Pumps

Water pumps are used to increase pressure in hydraulic systems, thus making the water flow. Pumps are typically the main actuators of a WSS and they can be either flow or pressure controlled. Therefore, pumps can have controllers to produce a desired flow or pressure. This is done by changing the rotational speed of the pump. In this way, when the pump has a reference pressure or flow, simple control makes it possible to produce the desired flow or pressure respectively [16].The pressure required to make the water reach some height is the sum of the pressure required to overcome the elevation and the friction losses in the pipe network.

The most common pumps in WSSs are centrifugal pumps. Normally, the characteristics of such pumps are described by two pump curves. The two curves depict the volume flow versus the pressure and the power of the pump respectively. Normally the curves describe the characteristics for one particular speed, which is denoted the nominal speed [16]. An example of these pump curves is shown in *Figure 2.4*.

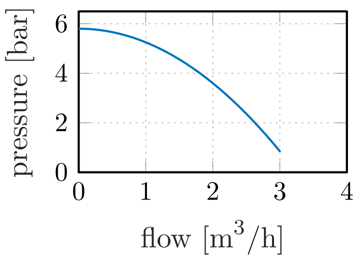

(a) Flow versus pressure difference

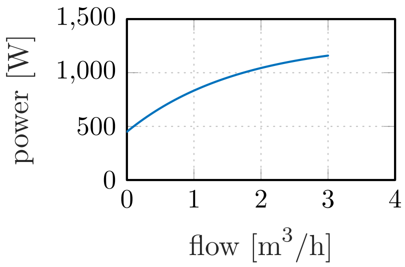

(b) Flow versus power consumption

Figure 2.4: Pump curves describing the performance of a centrifugal pump at nominal speed.

As can be seen, at a given flow, the pump can deliver a pressure with a maximum limit. This pressure decreases when the flow is increasing. At a certain flow and pressure value, the pump has an optimal point where the operation is the most energy efficient. Pumps are normally designed such that the optimal point lies in the operational area for the pumping application [9].

As in almost all WSSs, the flow is varying in the system, according to the flow demand from the end-consumers. Therefore, when dealing with varying flow in the system, pumps are often placed parallel at the pump stations such that they can keep their optimum points. As the flow increases, more pumps get activated to keep the pressure constant [9].

2.1.4 Valves

Valves in the WSS can be also seen as actuators along with pump elements. Unlike the pumps, valves are passive actuators in the sense that they do not consume energy. In principle, there are many types of valves existing. They can be categorized as non-return valves, control valves, shut-off valves and the combination of the two former one. Non-return valves allow waterflow only in one direction, while control valves can either adjust the flow or the pressure on their two endpoints. The former category is typically called a Flow Control Valve(FCV), while the latter is called a Pressure Reducer Valve or Pressure Regulating Valve(PRV). Shut-off valves are important components of the network since they can change the structure of the system, when for example doing maintenance or just redirecting the flow. This project deals with all three types of valves.

Valves can be controlled such that no flow passes through. In these cases the valve is closed and thereby certain parts of the system can be isolated as mentioned above. Other possibility is that the valve is fully open. In such case the pressure drop between the two endpoints is experienced because of the friction loss of the valve.

2.2 The Randers water supply network

The Randers drinking WSS is managed by Verdo A/S, which is the main supplier of drinking water and heating to the city of Randers. Verdo supplies water to approximately 46.000 customers in Randers Municipality [17]. The WSS is a complex, looped configuration with many different distribution areas. The coverage of the distribution areas are shown in *Figure 2.5* below.

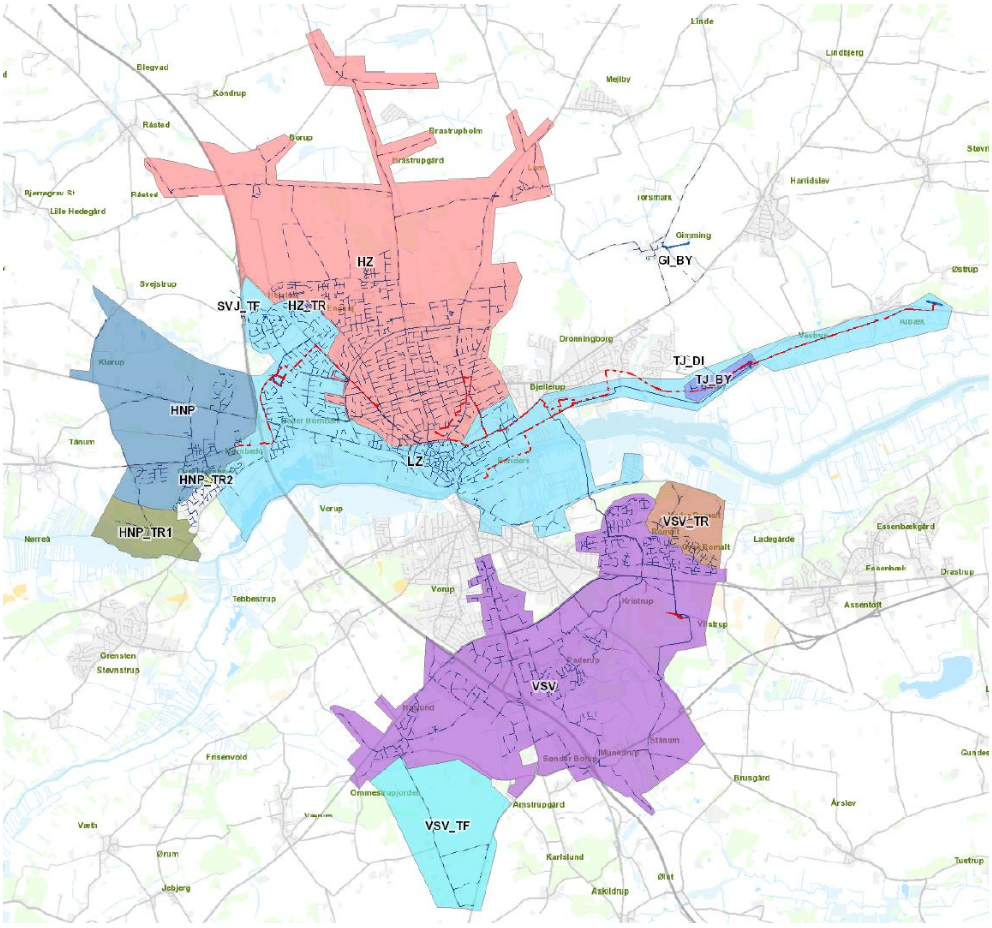

Figure 2.5: Distribution zones in the Randers WSS.

As can be seen in *Figure 2.5*, the network consists of many different distribution zones, however, the whole distribution map can be split into four main zones, according to the different geographical properties of the city. Furthermore, Randers is split into two regions, Randers North and Randers South. This is due to the fact that Randers fjord divides the city into two parts[17] .

The distribution network which is located in the southern part of the city is called Vilstrup zone. This zone has its own waterwork and pumping station which allows to supply the whole southern area by itself. This zone is shown in *Figure 2.6* below.

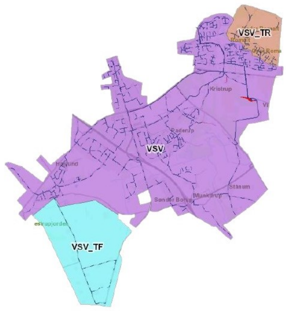

Figure 2.6: Vilstrup zone in Randers.

The only connection between Vilstrup and the northern region is through an emergency line, which is indeed used in emergency cases when the waterwork and pumping station in Vilstrup malfunctions or if there is a pollution in the WTs. In these cases waterworks from the northern parts can provide water to the Vilstrup zone. Besides the emergency cases, Vilstrup does not rely on the waterworks and pumping stations in Randers North.

Randers North consists of three different areas, each having its own particular geographical property. The water distribution in these regions are normally relies on each other, meaning that during a certain time period, the schedulings of the pumps are interconnected.

The area shown in *Figure 2.7* below is called the High Zone(HZ) due to the high elevation level of the region.

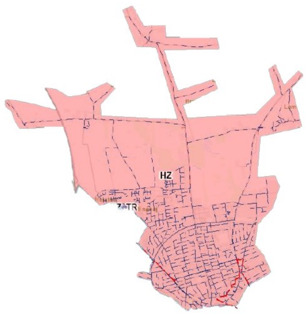

Figure 2.7: High Zone in Randers.

This part of the city lies approximately 55 meters above sea level, which means that big pumping effort is required to deliver the sufficient level of pressure to this area.

The area underneath the HZ is called the Low Zone(LZ). This zone in Randers lies approximately on sea level. Therefore, the HZ and LZ have a significant elevation difference which requires special pumping solutions in this area. In order to get a visual overview of the geographical properties of the HZ and LZ, the elevation profile is shown between these two areas in *Appendix: A*, in *Figure A.1* and *Figure A.2*. The area itself is shown in *Figure 2.8*.

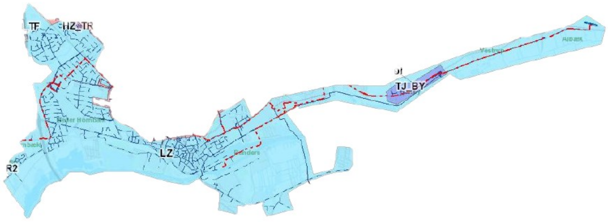

Figure 2.8: Low Zone in Randers.

The fourth main area in the Randers WSS is an area which according to its elevation neither belongs to the HZ, nor to the LZ. This area is called Hornbæk and shown in *Figure 2.9*.

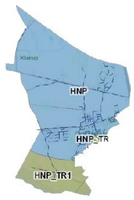

Figure 2.9: Hornbæk region in Randers.

The elevation in this area is around 30 meters above sea level and covers the western part of the city.

2.2.1 Waterworks and pumping stations

Verdo provides drinking water by pumping water from groundwater bases and treating the water in four different water works. Due to the high quality of ground water, this water treatment is only aeration in some cases. The WSS in Randers has four waterworks and four pumping stations, in different locations. In order to draw a better picture of the pumping and waterwork stations in the system, first they are listed and named and secondly their geographical locations and properties are described. The waterworks and pumping stations are the following

BKV	Bunkedal Waterwork
ØSV	Østrup Skov Waterwork
VSV	Vilstrup Waterwork
OMV	Oust Mølle Waterwork

Table 2.1: Waterworks in the network.

HBP	Hobrovej Pumping Station
HSP	Hadsundvej Pumping Station
TBP	Toldbodgade Pumping Station
HNP	Hornbæk Pumping Station

Table 2.2: Pumping stations in the network.

In order to show the geographical location of the waterworks and pumping stations in the network, an illustration of the network model is shown where each pumping station and waterwork are labelled with its name. The network is shown in *Figure 2.10*.

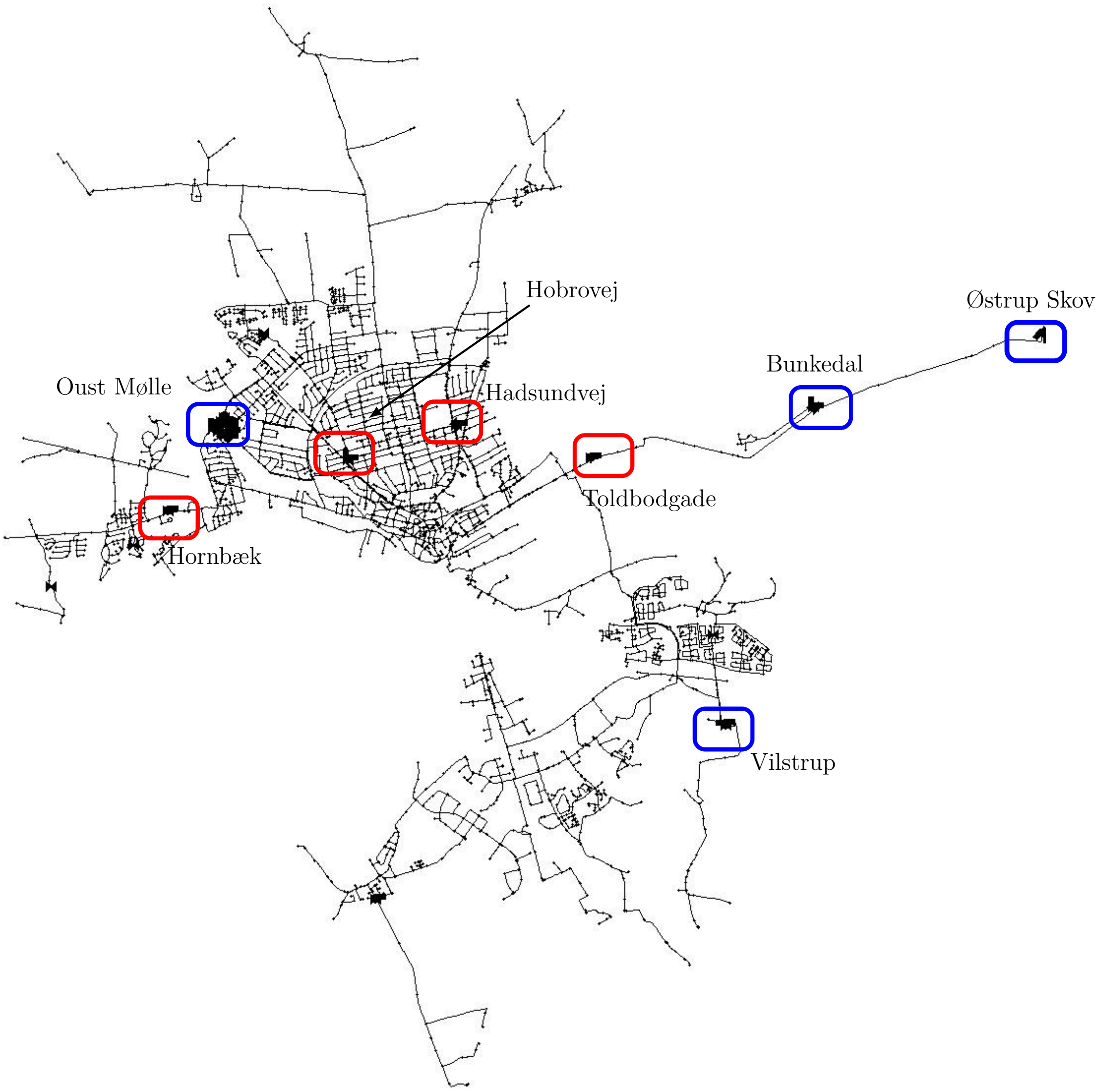

Figure 2.10: Waterworks(encircled in blue) and Pumping stations(encircled in red) in the Randers network.

The two main waterworks in the northern region are Bunkedal and Østrup Skov Waterworks. It is important to mention that in these areas, the water quality is sufficiently good, therefore clean water is pumped up to the surface. This is due to the fact that this groundwater lies under the ground such that it is protected by certain layers of the ground which makes it possible to provide this water without any kind of cleaning process, except aeration. These protection layers has been created by Randers fjord over the centuries due to glacial erosion (cite).

One of the drawbacks, however, is that the fresh water is located in the LZ, therefore the water has to be pumped from BKV and ØSV to locations with higher elevation.

Since BKV and ØSV are the main sources to the HZ and LZ areas, in the worst case, water has to be pumped up approximately 55 meters above sea level. For this reason, the pumping station called Toldbodgade provides the sufficient amount of pressure to the HZ areas. In the HZ areas, at the border of LZ and HZ, there are two pumping stations, Hadsundvej and Hobrovej, which divides the water distribution in the HZ and LZ.

As can be seen in *Figure 2.10*, the network in the HZ is a grid structure. The two main pump stations, HSP and HBP provide the sufficient pressure and flow to the grid and to the LZ areas, such that they keep a balance in pressure and flow. Furthermore, there is a WT placed both at HSP and HBP. Since the HZ has an elevation of approximately 55 meters, the static pressure in each WT at the two pumping stations is sufficient to provide pressure in the LZ areas, without any pumping effort. Therefore HSP and HBP provide pressure to the LZ areas such that the geodesic properties are exploited. An illustration of the two pumping stations and the HZ grid is shown in *Figure 2.11*.

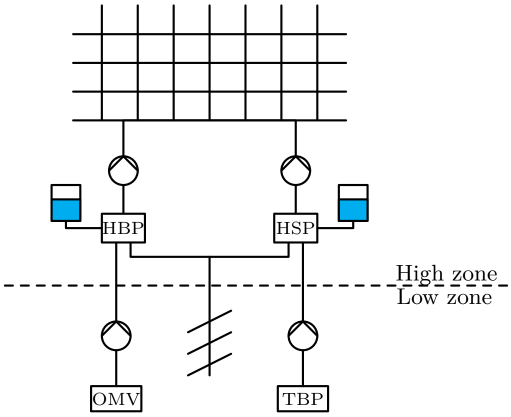

Figure 2.11: Hadsundvej and Hobrovej pumping stations with the HZ grid and LZ.

In order to avoid too high or too low pressure in the system, the pressure needs to be controlled alongside the flow. HBP is responsible for flow control, while HSP is responsible for the pressure control. Thereby it is avoided to provide the desired flow to the end-users with possibly with too high or too low pressure.

Furthermore, in Hornbæk zone, the elevation is above sea level, and the static pressure from the two main pumping stations can not provide the desired pressure to this region. Therefore, boosting is needed which is supplied by the Oust Mølle Waterwork and the Hornbæk Pumping Station. OMV and HNP thereby are responsible for the Hornbæk zone.

As it is described in Section *2.2: The Randers water supply network*, the Vilstrup zone is an individual distribution network, if normal operation is assumed. Therefore, the Vilstrup Waterwork is able to provide all flow demands in Randers South, without the help of the other waterworks in Randers North. Due to this consideration, the WSS in Randers South can be discarded when the control of Randers North is analysed.

In this report, the control of the two main pumping stations, Hadsundvej and Hobrovej is taken into account. This means that the Vilstrup region is indeed ignored, and the end-users are considered in the HZ, LZ and in Hornbæk region. With these considerations, the network simplifies to the following shown in *Figure 2.12*

Figure 2.12: The simplified network map of the Randers WSS.

The modelling of this system is going to be used for control purposes, which means that the model needs to be simple, but at the same time needs to have the same characteristics as of the original network. In the WSS in Randdders, the control purpose is to find an optimal control scheme which is able to actuate the pumps at the two main pumping stations, such that the dynamic effect of the WTs at each station are taken into account.

Tom's comments:
-some additional info on the purpose of the control
-what challenges should we face while controlling such system, with WTs included

3. System Modelling

This chapter gives a mathematical description of the component modelling. Thus, the different physical and mathematical measures of hydraulic systems are introduced. The similarities to electronic networks are shown by explaining the relevant properties of graph theory. A reduced model for multi-inlet networks is first introduced, then the inclusion of tanks is considered. In the end, the EPANET-based modelling approach is introduced and the proposed models are verified on simple pipe networks by comparing them to simulation results in EPANET.

3.1 Hydraulic component modelling

In this section the mathematical relation between pressure and flow is given for each component in a WSS system, in order to show their non-linear behaviour. The purpose here is not to derive the different models, but to introduce the mathematical formalism which describes them.

Equation: (3.1) shows the dual variable which describes all two-terminal components in the network

$$\begin{pmatrix} \Delta p \\ q \end{pmatrix} = \begin{pmatrix} p_{in} - p_{out} \\ q \end{pmatrix}, \tag{3.1}$$

where

Δp	is the differential pressure across the element,	[Pa]
q	is the flow through the element,	$\left[\frac{\mathrm{m}^3}{\mathrm{s}}\right]$
p_{in}, p_{out}	are the absolute pressures.	[Pa]

3.1.1 Hydraulic head

As can be seen in *Equation: (3.1)*, the measure of pressure is in $[Pa]$ and the measure of volumetric flow is in $[\frac{m^3}{s}]$. In the further report, the units used for calculation are in SI, however sometimes results are shown in non-SI units. Non-SI units are considered due to the fact that EPANET uses meter head and liters instead of pascals and cubic meters for pressure and flow simulations, respectively. The unit conversion between liters and cubic meters is a constant, however meter head expresses pressure in terms of length. The link between pressure and pressure head is explained in *Equation: (3.2)* below.

$$h_p = \frac{p}{\rho g}. \tag{3.2}$$

where

h_p	is the pressure head,	[m]
p	is the absolute pressure pascals,	$\left[\frac{\mathrm{kg}}{\mathrm{ms}^2}\right]$
g	is the gravitational constant,	$\left[\frac{\mathrm{m}}{\mathrm{s}^2}\right]$
ρ	is the density of the fluid.	$\left[\frac{\mathrm{kg}}{\mathrm{m}^3}\right]$

As can be seen in *Equation: (3.2)*, if the density of the liquid is a known parameter, the conversion can be made easily between pressure and pressure head. In this project, water is considered and its density is assumed to be constant.

In general, the hydraulic head, or total head, is a measure of the potential of fluid at a specific measurement point. It relates the energy of an incompressible fluid to the height of an equivalent static column of that fluid. The different forms of energies concerning fluids can be measured in distance, and therefore that is the reason that these terms are sometimes referred to as heads. The total hydraulic head of a fluid is composed of the pressure head and elevation head. [1]

The total head is given

$$h_t = h_p + z, \tag{3.3}$$

where

h_t	is the total head,	[m]
z	is the elevation(head).	[m]

Therefore, pressure head is a measurement of length, which is dependant on the density of the fluid but can be converted to the units of pressure. Using meters for describing pressure in the system is convenient for the reason, that pressure can be treated the same way as the elevation. In calculations, this property is exploited.

3.1.2 Pipe model

Pipes in the network are governed by the dynamic equation

$$\Delta p_i = J_i \dot{q}_i + f_i(q_i) - h_i, \tag{3.4}$$

where

J_i	is the mass inertia of the water in the pipes,
$f_i(q_i)$	is the pressure drop due to friction,
h_i	is the pressure drop due to geodesic level difference across the two terminals of pipe elements.

The dynamics of pipes due to mass inertia are discarded in this project, as it is shown in other works that the small time constant of these mass inertia dynamics are not dominant in the system, especially if there are elevated reservoirs included [9, 15]. Therefore the pressure drop across pipes can be written as

$$\Delta p_i = f_i(q_i) - h_i, \tag{3.5}$$

Additionally, the dynamics due to inertia of the liquid is not the only possible dynamics for pipes. The phenomenon, called water hammer occurs when a fluid, or gas in motion is forced to stop or change direction suddenly. In this case, a pressure wave runs through the pipe, causing vibration and possible damage in the network [19]. However, *Equation: (3.4)* models the pressure drops or equivalently, headloss, due to the elevation of the pipes and friction of the fluid. Therefore such rapid flow change is not assumed in the network.

The pressure drop due to friction across the i^{th} edge is a diagonal map where $f : \mathbb{R}^m \to \mathbb{R}^m$ is strictly increasing.[2] As it is shown in *Equation: (3.6)*, f_i describes a flow dependant pressure drop due to the hydraulic resistance such that

$$f_i(q_i) = \gamma_i |q_i| q_i, \tag{3.6}$$

[1] There is a third term, called the kinetic head which is discarded, since the velocity of the fluid is assumed to be constant along the cross sectional area in the whole length of pipes [18].

[2] A map $f : \mathbb{R}^m \to \mathbb{R}^m$ is strictly increasing if $\langle x - y, f(x) - f(y) \rangle > 0$ for every $x, y \in \mathbb{R}^m$ such that $x \neq y$ [20].

where

$\gamma_i > 0$	is the resistance coefficient, the parameter of pipes.	$[\cdot]$

Equation: (3.6) is motivated by turbulent flow in the pipes, which is typical in water supply applications. The resistance coefficient is calculated according to the Darcy-Weisbach formula, which provides the theoretically most precise result and is the most commonly used in Europe[8, 21]. γ is given as shown in *Equation: (3.7)* below[3].

$$\gamma(q) = \frac{c_D f_D(\epsilon, Re(q), D) l}{D^5}, \tag{3.7}$$

where

f_D	is the Darcy friction factor,	$[\cdot]$
ϵ	is the roughness of the pipe,	$[\mathrm{m}]$
D	is the diameter of the pipe,	$[\mathrm{m}]$
Re	is the Reynolds-number,	$[\cdot]$
c_D	is a coefficient in the D-W equation,	$\left[\frac{\mathrm{s}^2}{\mathrm{m}}\right]$
l	is the length of the pipe.	$[\mathrm{m}]$

In *Equation: (3.7)*, the Darcy friction factor, f_D, is dependant on the Reynolds number, which is defined by the volumetric flow in the pipes. However, at high flows Re becomes nearly constant and therefore normally this flow dependency is disregarded. Thus, f_D is considered to be constant in the further project.

The derivation of *Equation: (3.7)* is explained in more detail in appref [18]. Furthermore, in the following sections it is assumed that each f_i has a structure shown in *Equation: (3.6)*.

It is important to note here that $f_i(\cdot)$ is a homogeneous map which means that if the argument is multiplied by a positive scalar, then its value is multiplied by some power of this scalar [4]. For $f_i(q_i)$, it can be shown that

$$\gamma_i|(\alpha q_i)|(\alpha q_i) = f_i(\alpha q_i) = \alpha^2 f_i(q_i). \tag{3.8}$$

More precisely, with the given structure of $f(\cdot)$ the scaling would be $|\alpha|\alpha$, however $\alpha \geq 0$ is already assumed in *Equation: (3.8)*. This property is noted here and used later in the system description, in Section *3.4: Multi-inlet model*, where the scaling is indeed such that $\alpha \in \mathbb{R}_+$.

3.1.3 Valve model

Valves in the network are governed by the following algebraic expression

$$\Delta p_i = \mu_i(q_i, k_v) = \frac{1}{k_v(OD)^2}|q_i|q_i, \tag{3.9}$$

where

k_v	is the valve conductivity function, taking the Opening Degree(OD) of the valve in its argument [15].

$\mu_i(q_i, k_v)$ is a continuously differentiable and proper function which for $q_i = 0$ is zero and monotonically increasing.

3.1.4 Pump model

Centrifugal pumps are governed by the following expression [16]

[3] EPANET uses the D-W formula for calculating the resistance terms.
[4] $g(\alpha v) = \alpha^k g(v)$

$$\Delta p = -a_{h2}{q_i}^2 + a_{h1}\omega_r q_i + a_{h0}{\omega_r}^2 \tag{3.10}$$

where

Δp	is the differential pressure produced by the pump,	[Pa]
a_{h2},a_{h1},a_{h0}	are constants describing the pump,	[$\cdot$]
ω_r	is the impeller rotational speed.	$\left[\frac{\mathrm{rad}}{\mathrm{s}}\right]$

The model described in *Equation: (3.10)*, works only for positive flows, therefore it is assumed that liquid cannot flow back to the pump.

3.1.5 Elevated reservoir model

In elevated reservoirs, the rate of change in the volume of the fluid inside the tank is equal to the volumetric flow at which water enters or leaves the tank. Since the pressure on the bottom is due to the cross sectional area of the tank and the amount of water in it, proportional relation can be set between the pressure and the flow in and out of the tank. The dynamics of such system can be described by a first order differential equation of the form

$$\dot{p}_i = -\tau_i\Big(\frac{p_i}{h_{l,i}}\Big)q_i \tag{3.11}$$

where

p_i	is the pressure at the node connected to the tank,	[Pa]
$h_{l,i}$	is the water level in the tank,	[m]
τ_i	is the parameter in terms of the cross sectional area and the pressure/water level ratio in the tank,	$\left[\frac{\mathrm{Pa}}{\mathrm{m}^3}\right]$
q_i	is the flow into the tank if $q_i < 0$ and flow out of the tank if $q_i > 0$.	$\left[\frac{\mathrm{m}^3}{\mathrm{s}}\right]$

As can be seen in *Equation: (3.11)*, in general, the parameter of the tank depends on the pressure and water level ratio, if the cross sectional are is not constant along the height of the tank. However, it is assumed that tanks have the same cross sectional areas in the entire height. Then *Equation: (3.11)* simplifies to

$$\dot{p}_i = -\tau_i q_i. \tag{3.12}$$

In this case the parameter of the tank is given by

$$\tau_i = \rho g \frac{1}{A_{wt,i}} \tag{3.13}$$

where

$A_{wt,i}$	is the cross sectional area of the i^{th} tank.	[m^2]

3.2 Graph-based network modelling

Most of the tools, used by Circuit Theory(CT), are developed based on Graph Theory(GT). A WSS can be modelled as a directed graph with the set of vertices, representing the water sources and consumption nodes, and the set of edges, representing pipes, pumps and valves.

In order to track the pressure and flow in the desired part of the network, the equation system of the network has to be solved for the corresponding edges and vertices. The whole network can be described by writing up the equations for all edges in the network, based on the mathematical modelling of the different components in the system, as shown in Section *3.1: Hydraulic component modelling*. However, in case of complex systems such as water networks for large cities, these systems of equations are difficult to handle individually and typically cannot be solved explicitly if the system consists of loops. Therefore the properties of GT are not only useful for setting up relations between flow and pressure, but to make the handling of algebraic constraints easier by exploiting the properties of linear algebra. Thereby making it convenient for implementing it in computer algorithms for iterative solving methods.

WSSs can be described by a directed and connected graph, such that [22]:

$$\mathcal{G} = \{\mathcal{V}, \mathcal{E}\}, \tag{3.14}$$

where

$\mathcal{G}$	is a directed and connected graph,
$\mathcal{V}$	is the set of vertices, where $\mathcal{V} = \{v_1, ..., v_n\}$,
$\mathcal{E}$	is the set of edges, where $\mathcal{E} = \{e_1, ..., e_m\}$.

3.2.1 Incidence matrix

The incidence matrix, H, of a connected graph, $\mathcal{G}$, is a matrix where the number of rows and columns correspond to the number of vertices and edges, respectively. Therefore $H \in \mathbb{R}^{n\times m}$. In case of hydraulic networks, edges are directed in order to keep track of the direction of the flow in the system.

$$H_{i,j} = \begin{cases} 1 & \text{if the } j^{th} \text{ edge is incident out of the } i^{th} \text{ vertex.} \\ -1 & \text{if the } j^{th} \text{ edge is incident into the } i^{th} \text{ vertex.} \\ 0 & \text{if the } j^{th} \text{ edge is not connected to the } i^{th} \text{ vertex.} \end{cases} \tag{3.15}$$

It is worth mentioning that the reduced incidence matrix can be obtained by removing any arbitrary row from H. Therefore H always has $(n-1)$ row rank. This statement is induced by the mass conservation in the network and explained in the following section, Section *3.3: Kirchhoff's and Ohm's law for hydraulic networks.*

3.2.2 Cycle matrix

Purely tree structure of a WSS is not common when complex distribution systems are considered. However, trees can be arbitrarily chosen from the underlying graph of the network.[5] A tree, $\mathcal{T}^*$, of a graph is a connected sub-graph where any two vertices are connected by exactly one path [23]. Therefore trees in the network can be represented as follows

$$\mathcal{T}^* = \{\mathcal{V}_{\mathcal{T}^*}, \mathcal{E}_{\mathcal{T}^*}\}. \tag{3.16}$$

A special case of connected tree sub-graphs is the spanning tree of the network. A spanning tree contains all the vertices of $\mathcal{G}$ and has no cycles, since it is a tree. A spanning tree of the network therefore can be represented as

$$\mathcal{T}^*_{span} = \{\mathcal{V}, \mathcal{E}_{\mathcal{T}^*}\} \tag{3.17}$$

In order to obtain a spanning tree, an edge has to be removed from each cycle. The removed edges are $\mathcal{G} - \mathcal{T}^*$, and called the chords of $\mathcal{T}^*$ with respect to $\mathcal{G}$. By adding a chord to $\mathcal{T}^*$, a cycle is created which is called a fundamental cycle. A graph is conformed by as many fundamental cycles as the number of chords [23].

The set of fundamental cycles correspond to the fundamental cycle matrix, B, such that the number of rows and columns are defined by the number of chords and edges,

[5] Recall that a tree with n vertices has $n-1$ edges [23].

respectively. The cycle matrix of the system is given by

$$B_{i,j} = \begin{cases} 1 & \text{if the } j^{th} \text{ edge belongs to the } i^{th} \text{ cycle and their directions agree.} \\ -1 & \text{if the } j^{th} \text{ edge belongs to the } i^{th} \text{ cycle and their directions are opposite.} \\ 0 & \text{if the } j^{th} \text{ edge does not belong to the } i^{th} \text{ cycle.} \end{cases} \tag{3.18}$$

3.3 Kirchhoff's and Ohm's law for hydraulic networks

In this project, the hydraulic system is considered to be an open network with pipes, valves, pumps and the storage tanks, where water is able to enter and leave the network at a subset of the vertices. For such system, Kirchhoff's vertex law, or equivalently Kirchhoff's current law(KCL), corresponds to conservation of mass in each vertex and described by

$$Hq = d, \tag{3.19}$$

where

$d \in \mathbb{R}^n$	is the vector of nodal demands, with $d_i > 0$ when demand flow is into vertex i and $d_i < 0$ when demand flow is out of vertex i.	$\left[\frac{\mathrm{m}^3}{\mathrm{s}}\right]$

Nodal demands are seen as the end-user consumption, which means that water is taken out from the network. The mass conservation corresponds to the fact that what is consumed from the system must also be produced. Due to mass conservation, there can be only $(n-1)$ independent nodal demands in the network

$$d_n = -\sum_{i=1}^{n-1} d_i. \tag{3.20}$$

As a matter of fact, *Equation: (3.20)* is not an additional constraint since it follows from *Equation: (3.19)*. This can be sown by using the knowledge that 1_n is the left kernel[6] of H.

In the further report, a distinction is made between inlet and non-inlet nodes. It is assumed that the demand at non-inlet nodes fulfil the following constraint

$$d_i \leq 0. \tag{3.21}$$

It is worth noting however, that in closed hydraulic networks the vertex law becomes

$$Hq = 0. \tag{3.22}$$

Ohm's law for hydraulic networks is expressed with the incidence matrix, when H^T is applied to the vector of absolute pressures, p. Important to point out that the description below in *Equation: (3.23)* is valid if edges of the underlying graph are considered as only pipe elements.

$$\Delta p = H^T p = f(q) - H^T h. \tag{3.23}$$

In *Equation: (3.23)*, the differential pressure is described across each edge in the network, taking into account the pressure loss due to friction, $f(q)$, and the pressure drop due to geodesic level differences, where $h \in \mathbb{R}^n$ is the vector of geodesic levels at each vertex expressed in units of potential, i.e. pressure. It is noted that the pressure loss, $f(q)$, the absolute pressure, p and the geodesic level h can be both considered in

[6]The kernel of matrix $A \in \mathbb{R}^{m \times n)}$ is $\{x \in \mathbb{R}^n | Ax = 0\}$.

units of meter. As mentioned in the previous section, handling Ohm's law for hydraulic systems in meter is convenient, since the elevation is already in meters.

3.4 Multi-inlet model

The system is a water network supplied from more than one pumping stations and the distribution is to several end-users. In the underlying graph therefore the nodes are pipe connections, with possible water demand from the end-users, and the edges are only pipes.

The aim of the modelling here is to obtain a reduced order network model which is able to capture the dependence of the measured output pressures, on the flows and pressures at the inlets. The inclusion of storage tanks is the next step of the model development, therefore it is described in a following section, in Section *3.5: Inclusion of elevated reservoirs.*

It is assumed that the inlet pressures and demands are measured. Furthermore, pressure measurement is available in certain parts of the remaining network, at the end-users. Considering generality, the model is described for c inlets, however it should be noted that regarding the Randers WSS, two inlet vertices are taken into account.

In order to put the system into a form which can handle the measured pressure dependencies on the control inputs, the underlying graph of the network is first partitioned. The n vertices of the graph are separated into two sets

$$\mathcal{V} = \{\bar{\mathcal{V}}, \hat{\mathcal{V}}\}, \tag{3.24}$$

where

$\hat{\mathcal{V}} = \{\hat{v}_1, ..., \hat{v}_c\}$ represents the vertices corresponding to the inlet points,

and

$\bar{\mathcal{V}} = \{\bar{v}_1, ..., \bar{v}_{n-c}\}$ represents the remaining vertices in the graph.

The partitioning for the m edges of the graph is being chosen such that

$$\mathcal{E} = \{\mathcal{E}_\mathcal{T}, \mathcal{E}_\mathcal{C}\}, \tag{3.25}$$

where

$\mathcal{E}_\mathcal{T} = \{e_{\mathcal{T},1}, ..., e_{\mathcal{T},n-c}\}$

and

$\mathcal{E}_\mathcal{C} = \{e_{\mathcal{C},1}, ..., e_{\mathcal{C},m-n+c}\}$.

The subsets regarding edges and the partitioning is chosen such that the sub-matrix, which maps edges in $\mathcal{E}_\mathcal{T}$ to vertices in $\bar{\mathcal{V}}$, is invertible. It is worth mentioning that such partitioning is always possible for connected graphs.

Therefore, the incidence matrix can be split into four sub-matrices, as shown in *Equation: (3.26)* below

$$H = \begin{pmatrix} \bar{H}_\mathcal{T} & \bar{H}_\mathcal{C} \\ \hat{H}_\mathcal{T} & \hat{H}_\mathcal{C} \end{pmatrix}, \tag{3.26}$$

where

$\bar{H}_\mathcal{T} \in \mathbb{R}^{(n-c)\times(n-c)}$ is the sub-matrix, mapping edges in $\mathcal{E}_\mathcal{T}$ to vertices in $\bar{\mathcal{V}}$,
$\bar{H}_\mathcal{C} \in \mathbb{R}^{(n-c)\times(m-n+c)}$ is the sub-matrix, mapping edges in $\mathcal{E}_\mathcal{C}$ to vertices in $\bar{\mathcal{V}}$,
$\hat{H}_\mathcal{T} \in \mathbb{R}^{c\times(n-c)}$ is the sub-matrix, mapping edges in $\mathcal{E}_\mathcal{T}$ to vertices in $\hat{\mathcal{V}}$,
$\hat{H}_\mathcal{C} \in \mathbb{R}^{c\times(m-n+c)}$ is the sub-matrix, mapping edges in $\mathcal{E}_\mathcal{C}$ to vertices in $\hat{\mathcal{V}}$.

It is worth noting that the only requirement for the edge partitioning is $\bar{H}_{\mathcal{T}}$ being invertible[7]. Furthermore, the set $\mathcal{T} = \{\mathcal{V}, \mathcal{E}_{\mathcal{T}}\}$ is not necessarily a tree of the underlying graph, it can be any form of graph that fulfils the invertibility requirements. The set here, $\mathcal{T}$, is not connected due to the requirement of $\mathcal{E}_{\mathcal{T}} \geq (n-1)$. For the multi-inlet case, $c > 1$, therefore $\mathcal{E}_{\mathcal{T}} = (n-c)$. However, one special case is given when $c = 1$, meaning that the network has only one inlet. In this case, $\mathcal{T}$ is indeed a spanning tree.

With the chosen partitioning, Kirchhoff's vertex law in *Equation: (3.19)* can be rewritten as

$$\bar{d} = \bar{H}_{\mathcal{T}} q_{\mathcal{T}} + \bar{H}_{\mathcal{C}} q_{\mathcal{C}}, \tag{3.27a}$$

$$\hat{d} = \hat{H}_{\mathcal{T}} q_{\mathcal{T}} + \hat{H}_{\mathcal{C}} q_{\mathcal{C}}, \tag{3.27b}$$

and Ohm's law in *Equation: (3.23)*, separating the pressure drops due to hydraulic resistance

$$f_{\mathcal{T}}(q_{\mathcal{T}}) = \bar{H}_{\mathcal{T}}^T(\bar{p} + \bar{h}) + \hat{H}_{\mathcal{T}}^T(\hat{p} + \hat{h}), \tag{3.28a}$$

$$f_{\mathcal{C}}(q_{\mathcal{C}}) = \bar{H}_{\mathcal{C}}^T(\bar{p} + \bar{h}) + \hat{H}_{\mathcal{C}}^T(\hat{p} + \hat{h}). \tag{3.28b}$$

Writing up *Equation: (3.28a)* and *Equation: (3.28b)* in matrix form, the following yields

$$\begin{pmatrix} f_{\mathcal{T}}(q_{\mathcal{T}}) \\ f_{\mathcal{C}}(q_{\mathcal{C}}) \end{pmatrix} = \underbrace{\begin{pmatrix} \bar{H}_{\mathcal{T}}^T & \hat{H}_{\mathcal{T}}^T \\ \bar{H}_{\mathcal{C}}^T & \hat{H}_{\mathcal{C}}^T \end{pmatrix}}_{\begin{pmatrix} \bar{H}^T & \hat{H}^T \end{pmatrix}} \begin{pmatrix} \bar{p} + \bar{h} \\ \hat{p} + \hat{h} \end{pmatrix} \tag{3.29}$$

As it is shown in *Equation: (3.29)*, the transposed incidence matrices can be written up as the two sub-matrices partitioned according to inlet and non-inlet nodes.

Now, defining a matrix Γ, in which the partitioning of the edges are the same as for the incidence matrix, H. Γ is defined as follows

$$\Gamma = \begin{pmatrix} -\bar{H}_{\mathcal{C}}^T \bar{H}_{\mathcal{T}}^{-T} & I \end{pmatrix} \tag{3.30}$$

It should be noted that the expressions in matrix Γ are of the same structure as the structure of a partitioned cycle matrix [23]. However, as mentioned, the set $\mathcal{T}$ does not define a spanning tree when $c > 1$, therefore matrix Γ is not a cycle matrix corresponding to any spanning trees. Multiplying H with Γ from the left-hand side

$$\Gamma H^T = \begin{pmatrix} -\bar{H}_{\mathcal{C}}^T \bar{H}_{\mathcal{T}}^{-T} & I \end{pmatrix} \begin{pmatrix} \bar{H}_{\mathcal{T}}^T & \hat{H}_{\mathcal{T}}^T \\ \bar{H}_{\mathcal{C}}^T & \hat{H}_{\mathcal{C}}^T \end{pmatrix} = \begin{pmatrix} 0 & -\bar{H}_{\mathcal{C}}^T \bar{H}_{\mathcal{T}}^{-T} \hat{H}_{\mathcal{T}}^T + \hat{H}_{\mathcal{C}}^T \end{pmatrix}. \tag{3.31}$$

Multiplying with Γ from the left in *Equation: (3.29)*

$$\begin{pmatrix} -\bar{H}_{\mathcal{C}}^T \bar{H}_{\mathcal{T}}^{-T} & I \end{pmatrix} \begin{pmatrix} f_{\mathcal{T}}(q_{\mathcal{T}}) \\ f_{\mathcal{C}}(q_{\mathcal{C}}) \end{pmatrix} = \begin{pmatrix} -\bar{H}_{\mathcal{C}}^T \bar{H}_{\mathcal{T}}^{-T} & I \end{pmatrix} \begin{pmatrix} \bar{H}_{\mathcal{T}}^T & \hat{H}_{\mathcal{T}}^T \\ \bar{H}_{\mathcal{C}}^T & \hat{H}_{\mathcal{C}}^T \end{pmatrix} \begin{pmatrix} \bar{p} + \bar{h} \\ \hat{p} + \hat{h} \end{pmatrix} \tag{3.32}$$

induces the following expression

$$f_{\mathcal{C}}(q_{\mathcal{C}}) - \bar{H}_{\mathcal{C}}^T \bar{H}_{\mathcal{T}}^{-T} f_{\mathcal{T}}(q_{\mathcal{T}}) = (\hat{H}_{\mathcal{C}}^T - \bar{H}_{\mathcal{C}}^T \bar{H}_{\mathcal{T}}^{-T} \hat{H}_{\mathcal{T}}^T)(\hat{p} + \hat{h}). \tag{3.33}$$

From *Equation: (3.27a)*, the vector $q_{\mathcal{T}}$, of flows in edges $\mathcal{E}_{\mathcal{T}}$ can be expressed

[7] $\exists\{\mathcal{V}, \mathcal{E}\} : \bar{H}_{\mathcal{T}}^{-1} \because rank(H) = (n-1)$ [23]

$$q_{\mathcal{T}} = -\bar{H}_{\mathcal{T}}^{-1}\bar{H}_{\mathcal{C}}q_{\mathcal{C}} + \bar{H}_{\mathcal{T}}^{-1}\bar{d}. \tag{3.34}$$

Therefore using *Equation: (3.34)*, *Equation: (3.33)* can be rewritten

$$f_{\mathcal{C}}(q_{\mathcal{C}}) - \bar{H}_{\mathcal{C}}^T\bar{H}_{\mathcal{T}}^{-T}f_{\mathcal{T}}(-\bar{H}_{\mathcal{T}}^{-1}\bar{H}_{\mathcal{C}}q_{\mathcal{C}} + \bar{H}_{\mathcal{T}}^{-1}\bar{d}) = (\hat{H}_{\mathcal{C}}^T - \bar{H}_{\mathcal{C}}^T\bar{H}_{\mathcal{T}}^{-T}\hat{H}_{\mathcal{T}}^T)(\hat{p} + \hat{h}). \tag{3.35}$$

Now expressing the vertex demands at non-inlet vertices, $\bar{d}$, such that

$$\bar{d} = -v\sigma \tag{3.36}$$

where

$\bar{d} \in \mathbb{R}^{n-c}$	is the vector of nodal demands in non-inlet vertices,
$\sigma \in \mathbb{R}_+$	is the total demand in the network, representing the total consumption of the end-users,
$v \in \mathbb{R}_{n-c}$	represents the distribution vector of nodal demands among the non-inlet vertices with the property $\sum_i v_i = 1$ and $v_i \in (0;1)$.

Furthermore, introducing a vector, $a_{\mathcal{C}}$, such that

$$q_{\mathcal{C}} = a_{\mathcal{C}}\sigma. \tag{3.37}$$

It is worth mentioning that such an $a_{\mathcal{C}}$ can always be defined in this manner as long as $\sigma \neq 0$.

Having $\bar{d}$ and $q_{\mathcal{C}}$ introduced as the linear function of the total demand, σ, *Equation: (3.35)* can be expressed such that

$$\begin{aligned} &f_{\mathcal{C}}(q_{\mathcal{C}}) - \bar{H}_{\mathcal{C}}^T\bar{H}_{\mathcal{T}}^{-T}f_{\mathcal{T}}(-\bar{H}_{\mathcal{T}}^{-1}\bar{H}_{\mathcal{C}}q_{\mathcal{C}} + \bar{H}_{\mathcal{T}}^{-1}\bar{d}) = \\ &f_{\mathcal{C}}(a_{\mathcal{C}}\sigma) - \bar{H}_{\mathcal{C}}^T\bar{H}_{\mathcal{T}}^{-T}f_{\mathcal{T}}(-\bar{H}_{\mathcal{T}}^{-1}\bar{H}_{\mathcal{C}}a_{\mathcal{C}}\sigma - \bar{H}_{\mathcal{T}}^{-1}v\sigma) = \\ &f_{\mathcal{C}}(a_{\mathcal{C}})\sigma^2 - \bar{H}_{\mathcal{C}}^T\bar{H}_{\mathcal{T}}^{-T}f_{\mathcal{T}}(-\bar{H}_{\mathcal{T}}^{-1}\bar{H}_{\mathcal{C}}a_{\mathcal{C}} - \bar{H}_{\mathcal{T}}^{-1}v)\sigma^2. \end{aligned} \tag{3.38}$$

where the latter equality is due to the homogeneity property of the pressure drops due to frictions, previously explained in Section *3.1.2: Pipe model*.

Defining a function $F_v : \mathbb{R}^{m-n+c} \to \mathbb{R}^{m-n+c}$, parametrized with v such that it takes $a_{\mathcal{C}}$ as input, the following expression can be formed

$$F_v(a_{\mathcal{C}}) = f_{\mathcal{C}}(a_{\mathcal{C}}) - \bar{H}_{\mathcal{C}}^T\bar{H}_{\mathcal{T}}^{-T}f_{\mathcal{T}}(-\bar{H}_{\mathcal{T}}^{-1}\bar{H}_{\mathcal{C}}a_{\mathcal{C}} - \bar{H}_{\mathcal{T}}^{-1}v) \tag{3.39}$$

Furthermore, $F_v(\cdot)$ equals to the following, according to *Equation: (3.35)*

$$F_v(a_{\mathcal{C}}) = \frac{1}{\sigma^2}(\hat{H}_{\mathcal{C}}^T - \bar{H}_{\mathcal{C}}^T\bar{H}_{\mathcal{T}}^{-T}\hat{H}_{\mathcal{T}}^T)(\hat{p} + \hat{h}). \tag{3.40}$$

An algebraic expression for a_c can be found iff $\exists F_v^{-1}(\cdot)$. It can be shown, however that $\exists F_v^{-1}(\cdot)$ by showing that $F_v(\cdot)$ is a homeomorphism[8], which is done in [20].

As a result of using the inverse mapping of F_v, a unique expression can be obtained for $a_{\mathcal{C}}$

$$a_{\mathcal{C}} = F_v^{-1}A_1(\hat{p} + \hat{h}), \tag{3.41}$$

[8]Two functions are homeomorphic if they can be formed into each other by continuous, invertible mapping [24]. However, here invertibility is a sufficient condition.

where
$A_1 = \hat{H}_{\mathcal{C}}^T - \bar{H}_{\mathcal{C}}^T \bar{H}_{\mathcal{T}}^{-T} \hat{H}_{\mathcal{T}}^T \in \mathbb{R}^{(m-n+c \times c)}$.

A_1 has a non-trivial kernel, and for every unique value of $\frac{1}{\sigma^2} A_1(\hat{p}+\hat{h})$, there is a unique solution for $a_{\mathcal{C}}$.

The main objective of writing up $a_{\mathcal{C}}$ is to show that it can be expressed in terms of $v, \sigma(t), \hat{p}(t)$ and $\hat{h}$, where $\hat{h}$ and $\sigma(t)$ are assumed to be known signals and parameters, $v(t)$ is an unknown parameter and $\hat{p}(t)$ is the control signal. The difficulty about the constraint on $a_{\mathcal{C}}$ in *Equation: (3.41)* is that its structure is unknown. Equivalently, the solution for $a_{\mathcal{C}}$ cannot be expressed analytically but there exists a unique numerical solution for it.

Furthermore, assuming that $(\hat{p} + \hat{h}) \neq 0 \in \ ker(A_1)$, then $a_{\mathcal{C}}$, *Equation: (3.40)* can be simplified such that

$$a_{\mathcal{C}} = F_v^{-1}(0). \tag{3.42}$$

Equation: (3.42) shows, that in the special case when the input vertices are chosen such that the product $A_1(\hat{p} + \hat{h}) = 0$, then $a_{\mathcal{C}}$ becomes only dependent on the parameter v.

Now, using the equations for Ohm's law in *Equation: (3.28a)* and the vector $q_{\mathcal{T}}$, of flows in edges $\mathcal{E}_{\mathcal{T}}$ in *Equation: (3.34)*, the vector $\bar{p}$ of pressures at non-inlet vertices is expressed

$$\begin{aligned}\bar{p} =& \bar{H}_{\mathcal{T}}^{-T} f_{\mathcal{T}}(-\bar{H}_{\mathcal{T}}^{-1} \bar{H}_{\mathcal{C}} q_{\mathcal{C}} + \bar{H}_{\mathcal{T}}^{-1} \bar{d}) - \bar{H}_{\mathcal{T}}^{-T} \hat{H}_{\mathcal{T}}^T (\hat{p} + \hat{h}) - \bar{h} \\ =& \bar{H}_{\mathcal{T}}^{-T} f_{\mathcal{T}}(-\bar{H}_{\mathcal{T}}^{-1} \bar{H}_{\mathcal{C}} a_c + \bar{H}_{\mathcal{T}}^{-1} v)\sigma^2 - \bar{H}_{\mathcal{T}}^{-T} \hat{H}_{\mathcal{T}}^T (\hat{p} + \hat{h}) - \bar{h}\end{aligned} \tag{3.43}$$

As shown in *Equation: (3.43)*, the output vector which consists of the pressures in the non-inlet vertices can be written up in terms of $\sigma(t)$, $\hat{p}(t)$ time-varying signals, in terms of $\hat{h}$ and $\bar{h}$ constants and in terms of the parameter $a_{\mathcal{C}}$ and v. In the non-general case, as shown in *Equation: (3.42)*, a_c is a parameter which is governed by the behaviour of the total demand distribution among the non-inlet vertices. In case vector v is constant, thereby time-invariant, which means that the distribution of nodal demands are the same in all vertices in the network at all time, the output pressure in the i^{th} non-inlet vertices can be written as follows:

$$\bar{p}_i(t) = \alpha_i \sigma^2(t) + \sum_j \beta_{ij} \hat{p}_j(t) + \gamma_i \tag{3.44}$$

where
$\alpha_i = (\bar{H}_{\mathcal{T}}^{-T})_i f_{\mathcal{T}}(-\bar{H}_{\mathcal{T}}^{-1} \bar{H}_{\mathcal{C}} a_{\mathcal{C}} + \bar{H}_{\mathcal{T}}^{-1} v)$
$\beta_{ij} = -(\bar{H}_{\mathcal{T}}^{-T} \hat{H}_{\mathcal{T}}^T)_{ij}$
$\gamma_i = -(\bar{H}_{\mathcal{T}}^{-T} \hat{H}_{\mathcal{T}}^T)_i \hat{h} - \bar{h}_i$

However in WSSs, the above-mentioned consideration for v is unrealistic, meaning that the distribution of nodal demands in the non-inlet vertices should depend on time, as the end-user water consumption is not the same in every hour. This consumption behaviour of the end-users, however, is assumed to be periodic, which is a fair assumption, taking into account that the daily consumption shows approximately the same trends every day.

Therefore the demand in non-inlet vertices, described in *Equation: (3.36)* can be rewritten such that

$$\bar{d}(t) = -v(t)\sigma(t) \tag{3.45}$$

where
$v(t+T) = v(t)$,
$\sigma(t+T) = \sigma(t)$,
and T is the length of the period.

If the non-inlet demands are time-varying, but periodic behaviour is assumed and on top of this, the input vertices are arranged such that *Equation: (3.42)* is fulfilled, *Equation: (3.46)* can be rewritten as follows

$$\bar{p}_i(t) = \alpha_i(t)\sigma^2(t) + \sum_j \beta_{ij}\hat{p}_j(t) + \gamma_i, \tag{3.46}$$

where α_i is also a time-varying parameter of the model.

3.4.1 Simulation example

In order to illustrate and to show how the implementation of the model described in Section *3.4: Multi-inlet model* works, it is first tested on a simple, two-source, two-loop pipe network. This simple pipe system serves as an example to point out the differences and possible simplifications which were done regarding the modelling in Matlab and in EPANET. In this case, simulation results are steady-state values of pressures and flows, and the models are excited by some arbitrary pressure inputs.

The underlying graph of the example network is shown in *Figure 3.1*

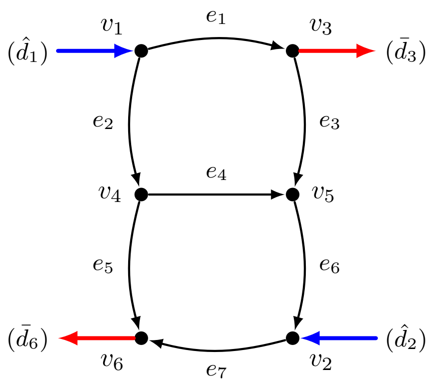

Figure 3.1: Graph of a simple multi-inlet network.

In *Figure 3.1*, arrows illustrate the in-and outflows such that input flows are present in v_1 and v_2, and user-consumption is defined only in v_3 and v_6. The diameters are the same for all pipes, however regarding the length, there are two types of pipes in this network. The corresponding parameters of the pipes, pumps, the elevation profile and the hourly demand variation is described in detail and can be found in (appref).

The partitioning of edges in the network is chosen such that

$$\mathcal{E}_\mathcal{T} = \{e_1, e_5, e_3, e_4\} \equiv \{e_{\mathcal{T},1}, e_{\mathcal{T},2}, e_{\mathcal{T},3}, e_{\mathcal{T},4}\}, \tag{3.47}$$

and

$$\mathcal{E}_\mathcal{C} = \{e_2, e_6, e_7\} \equiv \{e_{\mathcal{C},1}, e_{\mathcal{C},2}, e_{\mathcal{C},3}\}, \tag{3.48}$$

The corresponding vectors describing the pressures and flows in vertices and edges, respectively, furthermore the elevation and distribution profiles are given such that

$$p(t) = \begin{pmatrix} \bar{p}_3(t) \\ \bar{p}_4(t) \\ \bar{p}_5(t) \\ \bar{p}_6(t) \\ \hat{p}_1(t) \\ \hat{p}_2(t) \end{pmatrix}, \quad d(t) = \begin{pmatrix} \bar{d}_3(t) \\ 0 \\ 0 \\ \bar{d}_6(t) \\ \hat{d}_1(t) \\ \hat{d}_2(t) \end{pmatrix}, \quad h = \begin{pmatrix} \bar{h}_3 \\ \bar{h}_4 \\ \bar{h}_5 \\ \bar{h}_6 \\ 0 \\ 0 \end{pmatrix}, \quad v = \begin{pmatrix} v_3 \\ 0 \\ 0 \\ v_6 \end{pmatrix}. \tag{3.49}$$

From this arrangement of the edges and nodes, it follows that the sub-matrix, $\bar{H}_{\mathcal{T}}$, which maps non-inlet vertices to edges in set $\mathcal{E}_{\mathcal{T}}$, is invertible.

Since there are two nodes in the system with demand, the total flow leaving the network can be written as

$$\sigma(t) = -\bar{d}_3(t) - \bar{d}_6(t). \tag{3.50}$$

Having the input pressures and the parameters of the network, the output pressures, i.e. the pressures in the non-inlet vertices can be calculated. However, first recall *Equation: (3.35)*,

$$g(q_{\mathcal{C}}) = f_{\mathcal{C}}(q_{\mathcal{C}}) - A_1(\hat{p} + \hat{h}) + A_2 f_{\mathcal{T}}(A_3 q_{\mathcal{C}} + A_4 \bar{d}) = 0. \tag{3.51}$$

where

$$A_1 = \hat{H}_{\mathcal{C}}^T - \bar{H}_{\mathcal{C}}^T \bar{H}_{\mathcal{T}}^{-T} \hat{H}_{\mathcal{T}}^T,$$
$$A_2 = -\bar{H}_{\mathcal{C}}^T \bar{H}_{\mathcal{T}}^{-T},$$
$$A_3 = -\bar{H}_{\mathcal{T}}^{-1} \bar{H}_{\mathcal{C}},$$
$$A_4 = \bar{H}_{\mathcal{T}}^{-1}.$$

On account of non-linearity in *Equation: (3.51)*, it is not possible to solve the network analysis problem analytically. Instead, iterative numerical solution methods are used. As $g(q_{\mathcal{C}})$ is differentiable with respect to $q_{\mathcal{C}}$, gradient-based root finding algorithms such as Newton-Raphson method can be used. With iterative methods, initial values of flows are repeatedly adjusted until the difference between two successive iterates is within an acceptable tolerance. Furthermore, we know from the homogeneity and monotonicity property of $g(q_{\mathcal{C}})$ that the function is a homeomorphism in $q_{\mathcal{C}}$, therefore its root is unique. Using gradient-based searching methods, and squaring $g(q_{\mathcal{C}})$

$$2\frac{\partial g^T(q_{\mathcal{C}})}{\partial q_{\mathcal{C}}} g(q_{\mathcal{C}}) = 0, \tag{3.52}$$

the unique solution can be found. Furthermore, if $g^T(q_{\mathcal{C}})g(q_{\mathcal{C}})$ is convex, the solution is the global minimum. By solving *Equation: (3.51)* for $a_{\mathcal{C}}$, the non-inlet pressures and all flows in the network can be calculated in terms of the input pressures and the total demand in the network. In order to obtain these values, the previously-derived output equation in *Equation: (3.46)* can be used.

In the simulation, the most simple case is considered, when the total flow demand in the network varies, however the distribution among vertices remains the same. In this case, v is a constant vector, and the base demands in all vertices are the same.

The variation curve for the input pressures are set the same in both EPANET and in the simulator.

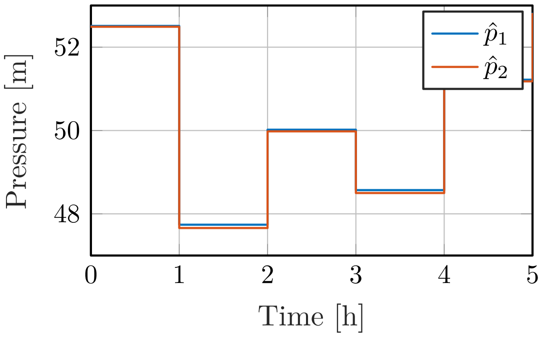

(a) Inlet pressures, ($\hat{p}$)

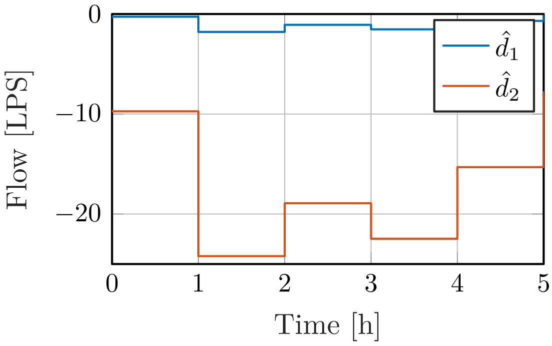

(b) Inlet demands, ($\hat{d}$)

Figure 3.2: Signals describing the input pressures(left) and flows(right) of the pumping stations.

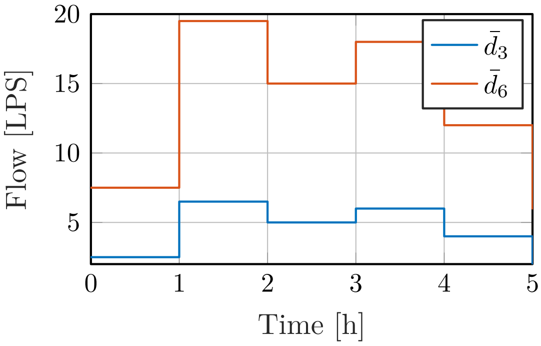

(a) Non-inlet demands, ($\bar{d}$)

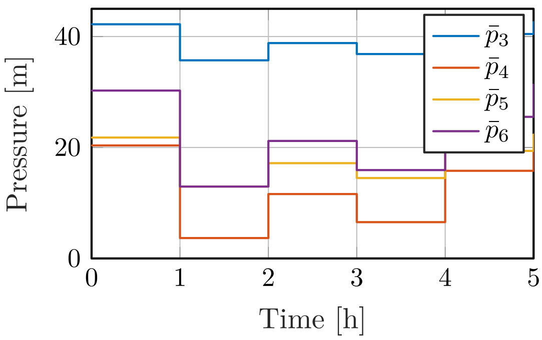

(b) Non-inlet pressures, ($\bar{p}$)

Figure 3.3: Signals describing the demand flows by the end-users(left) and output pressures(right) in the network.

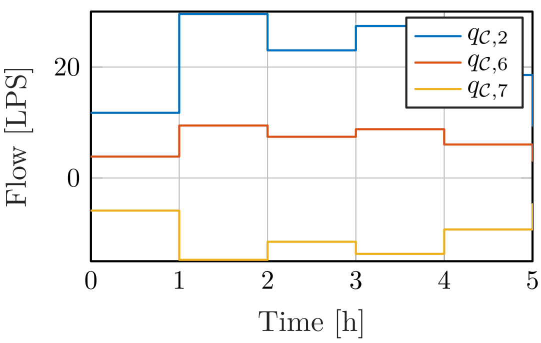

(a) Flows in $\mathcal{C}$, ($q_{\mathcal{C}}$)

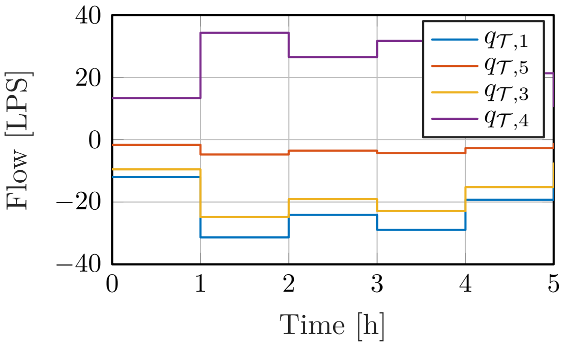

(b) Flows in $\mathcal{T}$, ($q_{\mathcal{T}}$)

Figure 3.4: Signals describing the flows in all pipes in the network.

3.5 Inclusion of elevated reservoirs

When a WT is being attached to an existing pipe network, certain properties of the previous system must be modified. Regarding the underlying graph of the network, when a WT is attached, the vertex to which the tank is connected becomes a vertex with a demand. However, the demand flow which describes the filling and emptying process of the tank, in this case, is not directly related to any user consumption profile, since flow can go into and come out of the tank. Therefore, the constraint on demand flows, described in *Equation: (3.21)* is not true in case of elevated reservoirs, as the demand can be both positive or negative. For this reason, demands on the reservoirs are treated as inputs and added to the nodes marked with hats $\hat{p}$ and $\hat{d}$. The nodes on which demand of elevated reservoirs are defined are selected from the input flows of the pumps such that

$$\hat{d} = F\hat{d}_t + G\hat{d}_c, \tag{3.53a}$$

where

$\hat{d}_t \in \mathbb{R}^{(l\times 1)}$ is the vector including the nodal demands of the tanks,
$\hat{d}_c \in \mathbb{R}^{(c\times 1)}$ is the the vector including the nodal demands of the pump inputs,
$F^T \in \mathbb{R}^{(l\times c+l)}$ is a mapping which selects the nodes belonging to tanks,
$G^T \in \mathbb{R}^{(c\times c+l)}$ is a mapping which selects the nodes belonging to pump inputs.

The same partitioning is done for the input pressures and elevation, regarding pumps and tanks

$$\hat{h} = F\hat{h}_t + G\hat{h}_c, \tag{3.53b}$$

$$\hat{p} = F\hat{p}_t + G\hat{p}_c, \tag{3.53c}$$

where

$\hat{h}_t \in \mathbb{R}^{(l\times 1)}$ is the vector including the elevation of the tanks,
$\hat{h}_c \in \mathbb{R}^{(c\times 1)}$ is the the vector including the elevation of the pump stations,
$\hat{p}_t \in \mathbb{R}^{(l\times 1)}$ is the vector including the absolute pressures in the tanks,
$\hat{p}_c \in \mathbb{R}^{(c\times 1)}$ is the the vector including the absolute pressures of the pump inputs.

With the inclusion of tanks, the network is not only constrained by the static pressure and flow relation, as in case of the model without tanks, but also governed by the dynamic equation describing the WT. These dynamics act as integrators on the flows which go in or out of the tank, $\hat{d}_t$. In terms of $\hat{d}_t$, the dynamics of the tanks set the pressure contribution, $\hat{p}_t$, as an input to the distribution system. The block diagram of such system is shown in *Figure 3.5*.

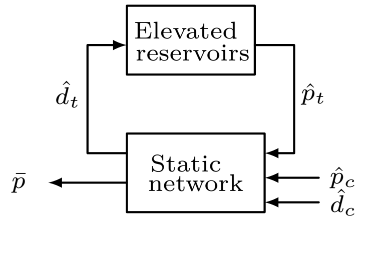

Figure 3.5: Block diagram of the system with WTs.

where the 'Elevated reservoirs' block represents the subsystem with dynamics, and the 'Static network' subsystem is governed by the algebraic flow and pressure relations which describe the pipe network.

When elevated reservoirs are introduced in the network, the system usually operates such that the control inputs are the flows, $\hat{d}$, as this is the most practical and robust way to control the network. In fact, this is the case regarding the Randers WSS, as the two pumping stations which are filling up the tanks are controlled by flow, as it was explained in Section *2.2.1: Waterworks and pumping stations*.

This modelling approach is different, however, from what is handled in case of a network without a tank, since instead of using the pressures, $\hat{p}$, the inlet flows, $\hat{d}_c$, are considered as inputs. Furthermore, regarding the dynamics, the filling and emptying of a tank is dependent on how much flow is delivered by the pumps. This inlet flow is provided by multiple pumping stations, however, a distinction has to be made between the presence of single or multiple WTs in the network. In the former case, the flows delivered by the pumps are filling or emptying the one and only tank in the network. In the latter case, however, the model needs to be able to handle the flow distribution among the different WTs, meaning that different pumping stations can have different filling or emptying effects on the different WTs. Therefore, in the following, the two different approaches are presented.

3.6 Multi-inlet, single-WT model

Recalling the dynamic equation of one tank, in *Equation: (3.12)*

$$\dot{\hat{p}}_t = -\tau \hat{d}_t, \tag{3.54}$$

it is seen that the flow, $\hat{d}_t$, needs to be expressed in terms of the inputs, $\hat{d}_c$. In order to express the demand regarding a tank, the whole network is treated as one node, as illustrated in *Figure 3.6*.

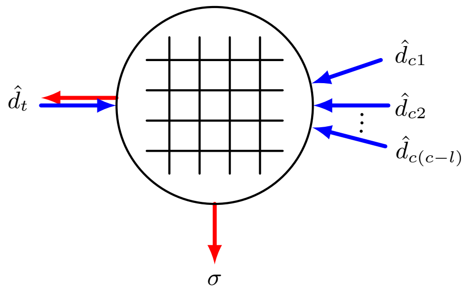

Figure 3.6: Mass balance on the network with one WT.

According to the mass-balance in the network, and using the corresponding partitioning as shown in *Figure 3.6*, the balance equation on all demand flows can be written in the form of

$$1^T d = 1^T \begin{pmatrix} \bar{d} \\ \hat{d} \end{pmatrix} = 1^T \begin{pmatrix} -\upsilon\sigma \\ \hat{d}_c \\ \hat{d}_t \end{pmatrix} = 0 \tag{3.55}$$

Now, expressing $\hat{d}_t$ from *Equation: (3.55)* yields

$$\hat{d}_t = \sigma - 1^T \hat{d}_c, \tag{3.56}$$

where it is shown, that if the control flows, $\hat{d}_c$, are higher than the total non-inlet demand, σ, the tank is being filled, and the tank is emptied if $\hat{d}_c$ is lower than σ. Thus, the system dynamics can be reformulated such that

$$\dot{\hat{p}}_t = -\tau(\sigma - 1^T \hat{d}_c). \tag{3.57}$$

It is important to point out that this first order differential equation in *Equation: (3.57)*, describes the mass-balance model of a single tank system, where the input flows equal to the overall demand in the network and the rate of change in storage in the tank. The result is not surprising, since according to *Equation: (3.57)*, the water level, or pressure, fluctuates according to the in- and outflow of water, which relates to the pumping effort and demand in the network.

In the single-WT modelling case, the dynamics can be described by a one-state, scalar equation, however the model is restricted to only one WT. As shown before, we know that this is not the case in the Randers WSS. Therefore, a more general description of the network is required, without restriction on the number of elevated reservoirs.

3.7 Multi-inlet, multi-WT model

In case when there are more than one WTs, the model based on the mass-balance equation, proposed in *Equation: (3.55)* is not applicable due to the fact that the pressures delivered by the tanks have to be balanced, similarly as in a simple connected-volume system. Therefore, a model framework is required which can handle the dynamics of multiple tanks, constrained by the static network and driven by the input flows of the pumping stations. In order to derive such model, the partitioning of the network is reconsidered. As described previously, the incidence matrix is partitioned such that

$$H = \begin{pmatrix} \bar{H}_{\mathcal{T}} & \bar{H}_{\mathcal{C}} \\ \hat{H}_{\mathcal{T}} & \hat{H}_{\mathcal{C}} \end{pmatrix}, \tag{3.58}$$

where $\bar{H}_{\mathcal{T}}$ is invertible. This partitioning rule on the edges is kept, however in the following model description let us slightly modify the notation and partitioning of the vertices. Now let

$$\mathcal{V} = \{\bar{\mathcal{V}}, \hat{\mathcal{V}}\}, \tag{3.59}$$

where

$\hat{\mathcal{V}} = \{\hat{v}_1, ..., \hat{v}_l\}$ represents the vertices corresponding to the points where elevated reservoirs are connected,

and

$\bar{\mathcal{V}} = \{\bar{v}_1, ..., \bar{v}_{n-l}\}$ represents the remaining vertices in the graph.

We originally defined $\bar{d}$ to describe non-inlet demands in the network and $\hat{d}$ to describe inlet-flows of the pumping stations, along with the demands of the WTs. With the redefined notation and partitioning of vertices, now we make sure that the vertices related to tanks are separated and all other points in the network are in the same set. So now, $\hat{d}$ describes flows regarding the WTs. In order to express the controlled inlet and non-inlet points in the network, the vectors related to the nodes marked with bars, $\bar{p}$ and $\bar{d}$, are split such that

$$\bar{p} = K\bar{p}_{\mathcal{K}} + D\bar{p}_{\mathcal{D}}, \tag{3.60a}$$

$$\bar{d} = K\bar{d}_{\mathcal{K}} + D\bar{d}_{\mathcal{D}}, \tag{3.60b}$$

where

$\bar{p}_\mathcal{K}$	is the vector including the inlet pressures ,
$\bar{p}_\mathcal{D}$	is the the vector including the non-inlet pressures,
$\bar{d}_\mathcal{K}$	is the the vector including the controlled inlet flows,
$\bar{d}_\mathcal{D} = -v_\mathcal{D}\sigma$	is the the vector including the non-inlet demands,
$K^T \in \mathbb{R}^{(c \times n-l)}$	is a mapping which selects the nodes belonging to the pumps,
$D^T \in \mathbb{R}^{(n-l-c \times n-l)}$	is a mapping which selects the nodes belonging to the rest of the network except pumps and elevated reservoirs.

With this partitioning of vertices, similarly to the model presented in Section *3.4: Multi-inlet model*, Kirchhoff's and Ohm's law can be formulated. Recalling Kirchhoff's vertex law

$$H \begin{pmatrix} q_\mathcal{T} \\ q_\mathcal{C} \end{pmatrix} = \begin{pmatrix} \bar{d} \\ \hat{d} \end{pmatrix}, \tag{3.61}$$

and recalling *Equation: (3.29)*, Ohm's law is given

$$\begin{pmatrix} f_\mathcal{T}(q_\mathcal{T}) \\ f_\mathcal{C}(q_\mathcal{C}) \end{pmatrix} = \begin{pmatrix} \bar{H}_\mathcal{T}^T & \hat{H}_\mathcal{T}^T \\ \bar{H}_\mathcal{C}^T & \hat{H}_\mathcal{C}^T \end{pmatrix} \begin{pmatrix} \bar{p} + \bar{h} \\ \hat{p} + \hat{h} \end{pmatrix}. \tag{3.62}$$

In order to get an expression for $\hat{d}$, describing the flows regarding the WTs, lets define matrix Ω as follows

$$\Omega = \begin{pmatrix} -\hat{H}_\mathcal{T}\bar{H}_\mathcal{T}^{-1} & I \end{pmatrix}. \tag{3.63}$$

Multiplying *Equation: (3.61)* with Ω from the left-hand side, $\hat{d}$ can be expressed in the form of

$$\hat{d} = (\hat{H}_\mathcal{C} - \hat{H}_\mathcal{T}\bar{H}_\mathcal{T}^{-1}\bar{H}_\mathcal{C})q_\mathcal{C} + \hat{H}_\mathcal{T}\bar{H}_\mathcal{T}^{-1}\bar{d}. \tag{3.64}$$

As shown in *Equation: (3.64)*, the vertex law describes the dependencies of the WT demands on $\bar{d}$, which now consists of the pump inlet flows and the non-inlet demands in the rest of the network, and also shows the dependencies on $q_\mathcal{C}$. Recalling and rewriting the equation governing elevated reservoirs in matrix form, we can write the following

$$\Lambda\dot{\hat{p}} = -\hat{d}, \tag{3.65}$$

where $\Lambda = diag(\frac{1}{\tau_1}, ..., \frac{1}{\tau_l}) \in \mathbb{R}^l_+$.

Inserting $\hat{d}$ in *Equation: (3.64)*, into the WT dynamics leads to

$$\Lambda\dot{\hat{p}} = -(\hat{H}_\mathcal{C} - \hat{H}_\mathcal{T}\bar{H}_\mathcal{T}^{-1}\bar{H}_\mathcal{C})q_\mathcal{C} - \hat{H}_\mathcal{T}\bar{H}_\mathcal{T}^{-1}\bar{d}. \tag{3.66}$$

Now, with the partitioning of $\bar{d}$, the inlet and non-inlet demands are inserted into *Equation: (3.66)*, resulting in the final governing expression of the dynamics

$$\Lambda\dot{\hat{p}} = -(\hat{H}_\mathcal{C} - \hat{H}_\mathcal{T}\bar{H}_\mathcal{T}^{-1}\bar{H}_\mathcal{C})q_\mathcal{C} - \hat{H}_\mathcal{T}\bar{H}_\mathcal{T}^{-1}K\bar{d}_\mathcal{K} + \hat{H}_\mathcal{T}\bar{H}_\mathcal{T}^{-1}Dv_\mathcal{D}\sigma. \tag{3.67}$$

As shown in *Equation: (3.67)*, the dynamics are now in terms of the inputs, $\bar{d}_\mathcal{K}$, the overall demand in the network, σ and $q_\mathcal{C}$. Recalling *Equation: (3.35)* in Section *3.4: Multi-inlet model* and using the abbreviations for the corresponding matrices, Ohm's law was reformulated such that

$$f_\mathcal{C}(q_\mathcal{C}) - A_1(\hat{p} + \hat{h}) + A_2 f_\mathcal{T}(A_3 q_\mathcal{C} + A_4\bar{d}) = 0. \tag{3.68}$$

Now, using again that $\bar{d} = K\bar{d}_{\mathcal{K}} + D\bar{d}_{\mathcal{D}}$, the following implicit expression is formulated which enables us to calculate $q_{\mathcal{C}}$

$$f_{\mathcal{C}}(q_{\mathcal{C}}) - A_1(\hat{p} + \hat{h}) + A_2 f_{\mathcal{T}}(A_3 q_{\mathcal{C}} + A_4 K\bar{d}_{\mathcal{K}} - A_4 D v_{\mathcal{D}}\sigma) = 0. \tag{3.69}$$

Along with the implicit expression for $q_{\mathcal{C}}$ in *Equation: (3.69)*, *Equation: (3.67)* describes the dynamics of the system, taking into account the static constraints by the demands. Therefore, the structure of the overall Multi-inlet, multi-WT model dynamics can be summarized as follows

$$\begin{cases} \Lambda\dot{\hat{p}}(t) = -(\hat{H}_{\mathcal{C}} - \hat{H}_{\mathcal{T}}\bar{H}_{\mathcal{T}}^{-1}\bar{H}_{\mathcal{C}})q_{\mathcal{C}}(t) - \hat{H}_{\mathcal{T}}\bar{H}_{\mathcal{T}}^{-1}K\bar{d}_{\mathcal{K}}(t) + \hat{H}_{\mathcal{T}}\bar{H}_{\mathcal{T}}^{-1}Dv_{\mathcal{D}}(t)\sigma(t), \\ f_{\mathcal{C}}(q_{\mathcal{C}}(t)) - A_1(\hat{p}(t) + \hat{h}) + A_2 f_{\mathcal{T}}(A_3 q_{\mathcal{C}}(t) + A_4 K\bar{d}_{\mathcal{K}}(t) - A_4 D v_{\mathcal{D}}(t)\sigma(t)) = 0. \end{cases} \tag{3.70}$$

Equation: (3.70) is a system of first-order Ordinary Differential Equations(ODE) with a constraint, specifying how the system evolves in time, given initial values of the states, $\hat{p}$, given the inputs, $\bar{d}_{\mathcal{K}}$, and parametrized by the time-varying parameter, $v_{\mathcal{D}}$. The constraint is set by the algebraic equations regarding the static network and includes information about the geometry on which the trajectory of the ODE solution can be found.

The states of the system are the pressures in the WTs, therefore when the model equations are solved for $q_{\mathcal{C}}$, initial information of the pressure values, $\hat{p}$, is required. Equivalently, the initial water levels in the tanks have to be known.

In order to calculate back the corresponding pressure inputs, $\bar{p}_{\mathcal{K}}$, first $\bar{p}$ is expressed from Ohm's law as proposed in Section *3.4: Multi-inlet model*

$$\bar{p} = \bar{H}_{\mathcal{T}}^{-T} f_{\mathcal{T}}(-\bar{H}_{\mathcal{T}}^{-1}\bar{H}_{\mathcal{C}}q_{\mathcal{C}} + \bar{H}_{\mathcal{T}}^{-1}\bar{d}) - \bar{H}_{\mathcal{T}}^{-T}\hat{H}_{\mathcal{T}}^{T}(\hat{p} + \hat{h}) - \bar{h}. \tag{3.71}$$

Now using that $\bar{p}_{\mathcal{K}} = K^T\bar{p}$, the pressure input equation becomes

$$\bar{p}_{\mathcal{K}} = K^T\bar{H}_{\mathcal{T}}^{-T} f_{\mathcal{T}}(A_3 q_{\mathcal{C}} + A_4 K\bar{d}_{\mathcal{K}} - A_4 D v_{\mathcal{D}}\sigma) - K^T\bar{H}_{\mathcal{T}}^{-T}\hat{H}_{\mathcal{T}}^{T}(\hat{p} + \hat{h}) - K^T\bar{h}. \tag{3.72}$$

Furthermore, using that $\bar{p}_{\mathcal{D}} = D^T\bar{p}$, the pressure output equation becomes

$$\bar{p}_{\mathcal{D}} = D^T\bar{H}_{\mathcal{T}}^{-T} f_{\mathcal{T}}(A_3 q_{\mathcal{C}} + A_4 K\bar{d}_{\mathcal{K}} - A_4 D v_{\mathcal{D}}\sigma) - D^T\bar{H}_{\mathcal{T}}^{-T}\hat{H}_{\mathcal{T}}^{T}(\hat{p} + \hat{h}) - D^T\bar{h}. \tag{3.73}$$

Equivalently, *Equation: (3.70)* and *Equation: (3.73)* can be described in a more abstract form, considering a non-linear state-space system structure such that

$$\begin{cases} \dot{\hat{p}} = g_{v_{\mathcal{D}}}(\bar{d}_{\mathcal{K}}, \sigma, q_{\mathcal{C}}) \\ \bar{p}_{\mathcal{D}} = h_{v_{\mathcal{D}}}(\hat{p}, \bar{d}_{\mathcal{K}}, \sigma, q_{\mathcal{C}}) \end{cases} \tag{3.74}$$
$$s.t. \quad q_{\mathcal{C}} = k_{v_{\mathcal{D}}}(\hat{p}, \bar{d}_{\mathcal{K}}, \sigma, q_{\mathcal{C}})$$

with $\hat{p} \in \mathbb{R}^l$ the state vector, $\bar{d}_{\mathcal{K}} \in \mathbb{R}^c$ the input vector, $\sigma \in \mathbb{R}_+$ the measurable disturbance and $v_{\mathcal{D}} \in \mathbb{R}^{(n-l-c)}$ the time-varying parameter.

It is worth noting here that this model with the flow inputs and the dynamics of the WTs results in a scalar dynamic equation in case of one tank. Therefore, the proposed restructuring of the model here is suitable for describing one tank systems as well, and capable of replacing the mass-balance based system dynamics, proposed in Section *3.6: Multi-inlet, single-WT model.*

3.7.1 Simulation example

Comments for supervisors:
Here the same kind of simulation is planned except that for this, water tanks will be considered. The simulation will be compared to the simulation in EPANET. Aim of this is to try the model, as for last time it helped me to find mistakes in unit conversion and in implementation. This part however has low priority now so it is planned to make it later. (It also helps to illustrate how the model is applied on a simple example network.)

3.8 Model comparison

In this chapter, three different model arrangements have been proposed and two of them have been derived for control purposes. As a summary of the network modelling, the different approaches and system structures are compared. It should be noted again, that notation has been redefined through the modelling, therefore symbols for the Multi-inlet and Multi-inlet, single-WT models are different from the one describing the Multi-inlet, multi-WT model. With this in mind, the properties of the three network models are summed up in the following table

	Multi-inlet model	**Multi-inlet/single-WT, based on mass-balance**	**Multi-inlet/multi-WT, general model**
Description	A model, describing a system without WTs, therefore describing a static network with time-varying parameters.	A model, describing the system dynamics with only one WT, relying on the mass-balance in the system, constrained by the static network. The parameter of the system is also time-varying.	A model describing the system dynamics with multiple WTs, constrained by the static network with time-varying parameter.
Input	$\hat{p}$ - Pressures of the multiple pumping stations.	$\hat{d}_c$ - Flows of the multiple pumping stations.	$\bar{d}_{\mathcal{K}}$ - Flows of the multiple pumping stations.
States	-	$\hat{p}_t$ - The pressure in one tank.	$\hat{p}$ - The pressures in multiple tanks.
Output	$\bar{p}$ - Pressures in the non-inlet points.	$\bar{p}$ - Pressures in the non-inlet points	$\bar{p}$ - Pressures in the non-inlet points.
Advantages	The network is without dynamics, therefore all solutions are steady-state values.	The network is controlled with flow, which makes the system more robust towards pressure errors in the WT. The dynamics are governed by a scalar equation, relying on the input flows.	The control can handle the pressure balance among multiple WTs.
Governing equations	$\bar{p} = g_v(\hat{p}, \sigma, q_{\mathcal{C}})$ $q_{\mathcal{C}} = k_v(\hat{p}, \sigma, q_{\mathcal{C}})$	$\dot{\hat{p}}_t = e(\sigma, \hat{d}_c)$ + static network equations	$\begin{cases} \dot{\hat{p}} = g_{v_{\mathcal{D}}}(\bar{d}_{\mathcal{K}}, \sigma, q_{\mathcal{C}}) \\ \bar{p}_{\mathcal{D}} = h_{v_{\mathcal{D}}}(\hat{p}, \bar{d}_{\mathcal{K}}, \sigma, q_{\mathcal{C}}) \end{cases}$ $q_{\mathcal{C}} = k_{v_{\mathcal{D}}}(\hat{p}, \bar{d}_{\mathcal{K}}, \sigma, q_{\mathcal{C}})$
Section reference	Section *3.4: Multi-inlet model*	Section *3.6: Multi-inlet, single-WT model*	Section *3.7: Multi-inlet, multi-WT model*

Table 3.1: Summary of the network models.

In the further discussion, the Multi-inlet, multi-WT network model is considered, as that one is the most suitable for describing the water network in Randers. Furthermore, the redefined notation is kept.

4. Simulation framework in EPANET

This chapter gives an insight into the simulation model of the Randers WSS in EPANET. In order to better understand how the simulation works, the modelling steps of the different pumping stations, waterworks, and the consumption patterns are explained in detail. In the end, an attempt is made to split the network into different subsystems and make necessary modifications such that data is easily extractable for system identification purposes.

4.1 Model and data structure

As it was explained in Chapter *2: Description of Water Supply Systems*, the typical components of WSSs are reservoirs, pipes, pumps and valves. Each of these interconnected elements are dependent on their neighbours, thus the behaviour of the entire WSS depends on each of its elements. For simulation purposes, it is required that the model of the real-life network consists of thousands of elements in order to accurately replicate hydraulic behaviour and the topographical layout of the system. Such models are appropriate for simulation purposes, however, online optimisation tasks are much more computationally demanding. Therefore the available data in the simulation framework is to be used to create a more compact model for control purposes.

The use of Geographic Information Systems(GIS) in the water industry resulted in an increasing amount of information about actual network topology and service that can be utilized in a model [25]. As a consequence of this, normally the simulation model of WSSs include exactly the same amount of components as in real-life.

The following data and model description strongly relies on the documentation of the Randers WSS EPANET model [26], provided by Verdo A/S, where the considerations and modelling steps with the available data from GIS are gathered. The model is mainly based on the data stored in GIS, however considerations on case studies and experience have also been taken into account. It is important to note that the following results and properties of the EPANET model serve as a basis for the data processing and therefore is discussed in the report.

Initially during the modelling, nodes were made among each different pipe elements, however this increased the calculation time significantly. Therefore the number of nodes in the network were reduced based on the fact that pipe sections with the same material and dimensions can be treated as one pipeline. In order to illustrate the complexity of the network, the number of elements in the simulation model including the VSV region, is shown in *Table: 4.1*

Element type	**Number**
Links	4144
Nodes	4180
Tanks	6

Table 4.1: Number of WSS elements.

It is important to note that the number of tanks in the model does not necessarily reflect the number of WTs in the real system. In certain parts of the system, the modelling reflects the real-world results, however the structure of certain pumping stations and waterworks are different. For the same reason, at some places in the simulation one pump serves to simulate a whole pumping station while in the real world more pumps are placed in parallel.

4.1.1 Water consumption data

In the model, consumption data is divided into two groups: non-industrial and industrial demands. The number of demand categories were chosen to keep down as it turned out that the quality of this data from GIS is not representative enough, as relatively few building addresses, which are the registered floor and two or more storey buildings. The consumption curves were defined such that they are matched the pumped water volumes from waterworks and pumping stations in each individual zones. Therefore a calculation for the deviation has been made over the day such that it was possible to conclude on the uniformity of the consumption types in each zone [26]. With around 3 percent uncertainty, the consumption patterns turned out to be reliable in the model. The demand patterns over a 24 hours long period are shown in

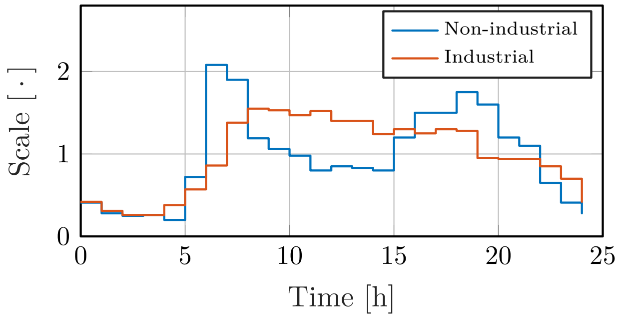

Figure 4.1: Industrial and Non-industrial demand patterns in the EPANET simulation.

It is worth noting that the industrial consumption profile in the VSV zone slightly differs from the industries in the rest of the network. However, since the VSV zone is not considered in the further simulation model, the demand pattern is not shown here. Furthermore, there are no consumers in the corresponding supply areas who have significant effect on water consumption such that it influences the model calibration and simulation.

4.1.2 Pump stations and waterworks

As described in Section *2.2: The Randers water supply network*, there are several different pumping stations and waterworks in the network, supplying different zones. In general, there is a possibility in EPANET to simulate the cleaning process in the waterworks, including drilling, raw water and clean water treatment, however in the model the focus is on the correct distribution. Therefore all waterworks are simulated with using clean water reservoirs with. In the EPANET simulation, pumps in the waterworks pump the water out corresponding to the real pump curves. However, there is one exception, where the simulation of the pumping station is different. In the OMV water work, which is responsible for filling the tank(T1) in HBP pumping station in the HZ, the precise operation of the pumping station has not been taken into account. Instead, the control schedule of the pumps has been simulated as a positive demand node(negative according to the EPANET sign convention), just as in the network modelling, proposed in this report. The reason for this is that the controls turned out to be relatively complicated with frequency converters and simulation results of the pumping were not matching the real world scenarios. The advantage of this is that in one of the flow controlled pumping stations, the mass balance is controlled and furthermore the risk that the model does not simulate correctly is reduced. Apart from the OMV water work, all water works have been simulated with reservoirs which cannot be emptied by calculation. Water works and pumping stations, where the pumps are pressure controlled, are controlled by PRVs, as this is the typical way of controlling pressure controlled pumps in EPANET networks [21]. Such an arrangement is shown in *Figure 4.5*

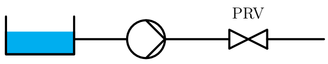

Figure 4.2: Water works modelled in EPANET, except OMV.

It is important to note, however that with this arrangement in case of high demands in the network it is possible that water works and pumping stations deliver more flow than is actually possible. Therefore control rules have been incorporated in the models which prevents the pumping stations produce more flow than available in the real world.

4.2 Model calibration and validation

The simulation data has been validated by using pressure measurements on different fire hydrants in the network for several times in different years. When the model was made, the data was not completely up to date, as these pressure measurements were carried out in years before the EPANET modelling. The major uncertainty about this data is in the arrangement of the pipe network and the pumping stations, since it has been changed over the years and old facilities have been replaced. Although the data on which the model relies is uncertain and there might be variations in pressure, the validation of the model has been carried out according to these highly uncertain pressure measurements.

4.2.1 Pipe roughness

In the model, all pipes are associated with tags, indicating dimensions, material and year information. With this information it is possible to estimate an average resistance, i.e. roughness of the pipes. During the validation process of the pipe resistances, it was chosen to consider an average roughness value, taking into account that the roughness should not be lower than a roughness of new pipes and at the same time, should not exceed a certain upper bound. Roughnesses were upscaled at places where the pressure was too high while downscaled where the pressure was certainly too low. Correct pressure data, however is an essential information for a more detailed and precise calibration, therefore high deviations are present in the system up to 5 meter heads.

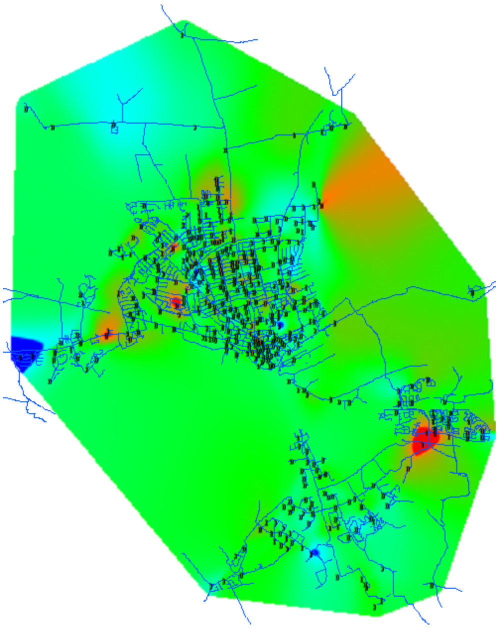

Figure 4.3: Difference calculation between observed and calculated pressures on fire hydrants[26].

4.2.2 Grid balance and supply zones

With the simulation model in EPANET it is possible to illustrate which pumping stations supply the different areas in the network. Simulations can be carried out for instance on supply areas in certain zones where more than one pumping station contributes to the consumption. The two zones, considered in this report are the HZ and LZ, in which the former is supplied by OMV and TBP and the latter is supplied by HBP and HSP where the tanks are placed on high elevation level. Consequently, as mentioned in Section *2.2.1: Waterworks and pumping stations*, OMV and TBP are the waterworks and pumping stations which are responsible for filling the tanks in the HZ in HBP and HSP, respectively. *Figure 4.4* shows the distribution between the two pumping stations, HBP and HSP, in the high zone.

(a) HSP supply area, marked with red (b) HBP supply area, marked with red

Figure 4.4: Supply area by HSP(on the left) and supply area by HBP(on the right)(cite).

The red areas in *Figure 4.4* indicate 80-100 percent of drinking water originating from one or the other pumping station. However, the other colours(primarily yellow and green) indicate that there is a mix of water from both stations. The result in the grid is according to the control goals, as one pumping station supplies half of the region and an other the other one. This is achieved by controlling the flow in HBP and the pressure in HSP.

4.3 Model preparation for data extraction

Discussion for supervisors for the meeting:
Concerns: The two pumping stations in the high zone. The aim of these pumping stations is to distribute water to the grid in the high zone with the help of the watertanks. In EPANET the control is set such that the supply is nearly 50-50 percent. How to incorporate the effect of these into the model from which the data is extracted, since the pumping stations for control are considered to be the two stations in the low zone. Or is it even necessary if we do black box modelling? In the figure below the illustration is shown for help:

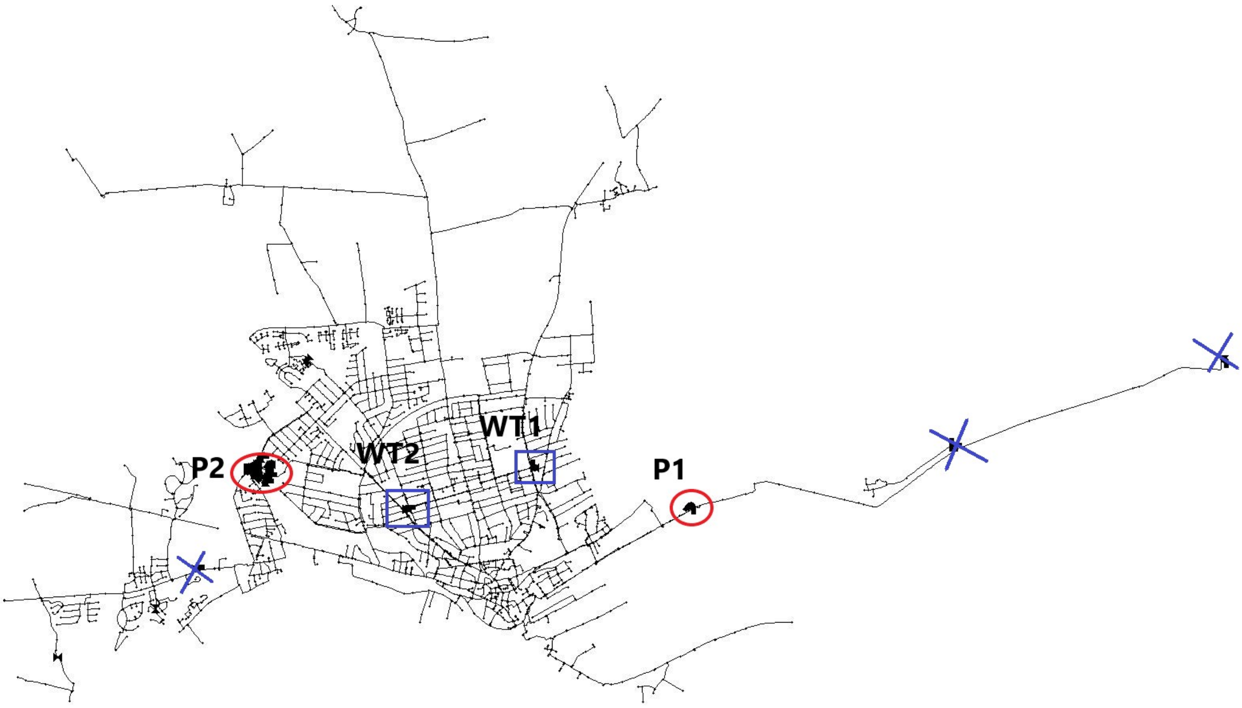

Figure 4.5: Illustration for helping the discussion.

When data is extracted for system identification, it has to be considered that the pumping effort on P1 and P2 is not that high because the two pumping stations in the grid help in the high zone.

Part II

System Identification

5. State of the art system identification analysis

In this chapter, first an overview is given about the different methods for non-linear system identification. Secondly, the chosen method for identification is discussed in detail putting focus on the structure of the network.

The data available in the simulation framework allows us to make a system model with the proposed control structure, however the complexity would be high. Try some black-box identification which can reproduce the same properties of the original simulation network but easier to handle in control.

Comments for supervisors:
The data that should be gathered for any kind of system identification:
σ - the overall consumption in the system in different time steps. For example for a 24 hours time period.
$\bar{p}_{\mathcal{D}}$ - pressure measurements in different non-inlet points.
$\hat{d}_{\mathcal{K}}$ - information about how the two main pumps actuated to get the output data
Along with this, in case of a neural-based network approach how the structure of the control model should be incorporated in the identification. Because in e grey-scale system identification approach, the information about the structure derived in the system model is considered.

Part III

Appendices

A. Elevation Profile from HZ to LZ

Figure A.1: Elevation profile along the High and Low Zones 1.

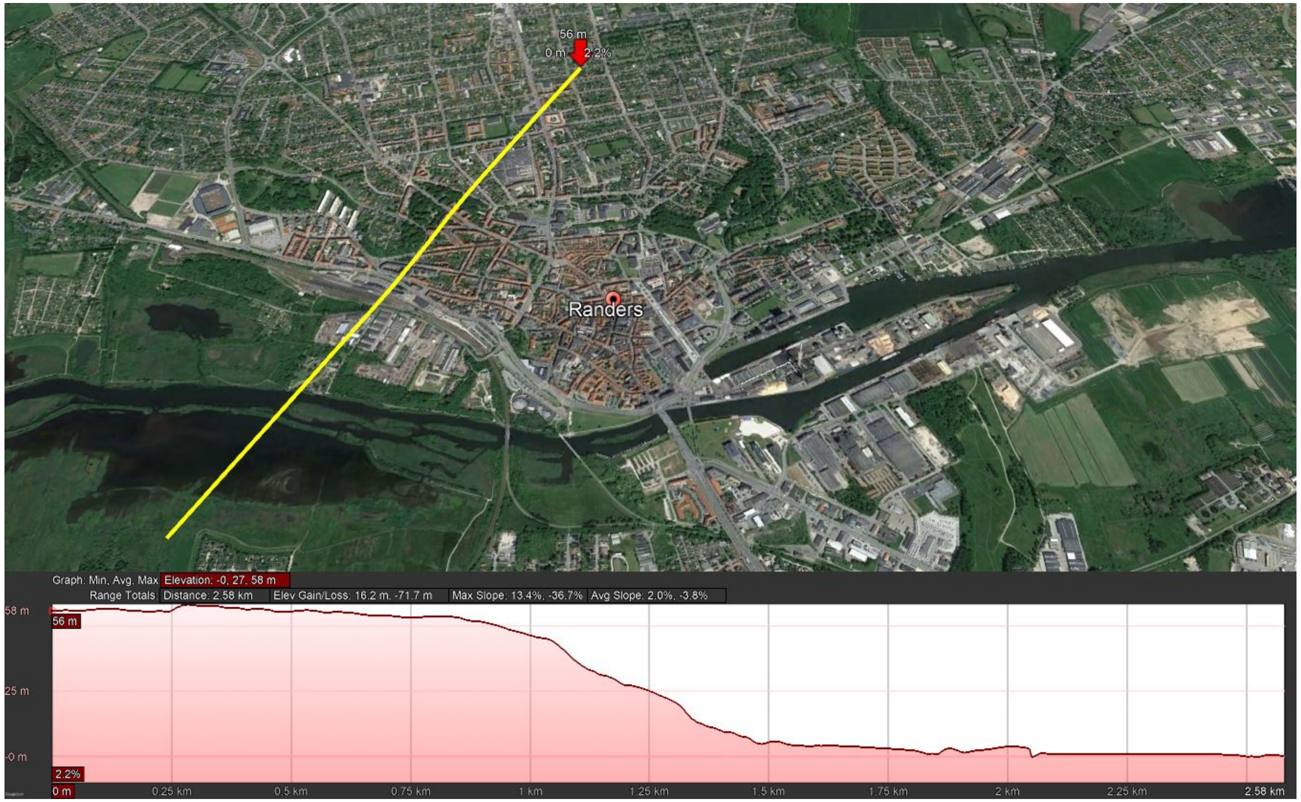

Figure A.2: Elevation profile along the High and Low Zones 2.

B. Assumption List

In this part of the appendix, the different assumptions and simplifications, which were applied in the project, are collected. In order to ease the reading, a reference points to the part in the report where the relevant assumption is used.

Number	**Assumptions**	**Section reference**
1	The fluid in the network is water.	Section *3.1.1: Hydraulic head*
2	All pipes in the system are filled up fully with water at all time.	Section *3.1.2: Pipe model*
3	The pipes have a cylindrical structure and the cross section, $A(x)$, is constant for every $x \in [0, L]$.	Section *3.1.2: Pipe model*
4	The flow of water is uniformly distributed along the cross sectional area of the pipe and the flow is turbulent.	Section *3.1.2: Pipe model*
5	The change in elevation, z, occurs only in pipes.	Section *3.1.2: Pipe model*
6	At high flows, the Reynolds number is assumed to be constant. Therefore the Darcy friction factor, f_D is assumed to be constant.	Section *3.1.2: Pipe model*
7	Pumps in the network are of the type centrifugal.	Section *3.1.4: Pump model*
8	Tanks in the network have constant diameters. Equivalently, walls of the tanks are vertical.	Section *3.1.5: Elevated reservoir model*
9	Functions describing the pressure drops regarding the flow through them across the components of the system are continuously differentiable.	Section *3.4: Multi-inlet model*

Table B.1: List of assumptions

C. Example Network

C.0.1 Simulation in EPANET

In EPANET, the simulation is built up in the same way as the network model. The simulation model is shown in the figure below.

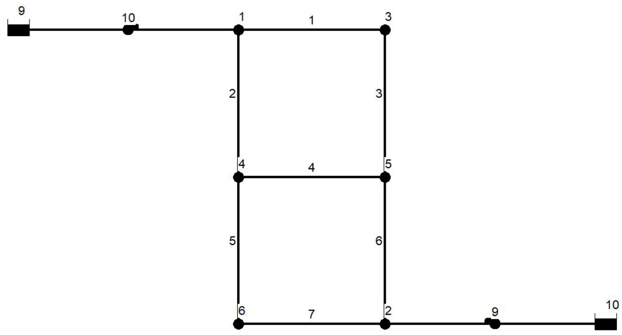

Figure C.1: Non-inlet pressures in .

As can be seen in *Figure C.1*, reservoirs and pumps are present as extra links and nodes in this simulation. These extra nodes and links are removed when data is extracted from the EPANET model due to the reason that the input pressures can be measured on v_1 and v_2. The input flows can be measured through the links, connecting the reservoirs to the nodes, v_1 and v_2. Furthermore, the elevations and the demands are attributes of the nodes. In this simulation only demands are changing according to hourly time steps.

D. Example Network with elevated reservoir

D.1 unspecified1

E. Measurements

Bibliography

[1] T. Younos and T. Parece, *Sustainable Water Management in Urban Environments*. The Handbook of Environmental Chemistry, Springer International Publishing, 2016.

[2] Y. X. J.N. Tsitsiklis, “Pricing of fluctuations in electricity markets,” *European Journal of Operational Research*, 2015.

[3] B. Appelbaum, “Water & sustainability (volume 4): Us electricity consumption for water supply & treatment—the next half century,” 2002.

[4] N. R. Council *et al.*, *Public Water Supply Distribution Systems: Assessing and Reducing Risks–First Report*. National Academies Press, 2005.

[5] Miljøministeriet and Geus, *Water Supply in Denmark*. Danish action plan for promotion of eco-efficient technologies - Danish Lessons, 2009.

[6] M. Brdys and B. Ulanicki, *Operational Control of Water Systems: Structures, Algorithms, and Applications*. Prentice Hall, 1994.

[7] M. Beniston, *Environmental Change in Mountains and Uplands*. Key Issues in Environmental Change, Taylor & Francis, 2016.

[8] P. Swamee and A. Sharma, *Design of Water Supply Pipe Networks*. Wiley, 2008.

[9] K. Hoe, “Modeling and control of water supply network,” *Danmarks Tekniske Universitet*, 2005.

[10] T. Walski and I. Haestad Methods, *Advanced water distribution modeling and management*. No. vb. 1, Haestead Press, 2003.

[11] M. MØlgaard and B. G. Pétursson, *Energy Optimization of Water Distribution Networks*. 2015. Master thesis, Aalborg University.

[12] N. Grigg, *Water, Wastewater, and Stormwater Infrastructure Management, Second Edition*. Taylor & Francis, 2012.

[13] L. Mays, “Water transmission and distribution,” *American Water Works Association, Denver*, 2010.

[14] N. Council, D. Studies, W. Board, and C. Risks, *Drinking Water Distribution Systems: Assessing and Reducing Risks*. National Academies Press, 2007.

[15] D. Andersen, K. Balla, N. Christensen, I. Bolinaga, and S. Krogh, *Optimal Control for Water Distribution*. Aalborg Universitet, 2017.

[16] C. Kallesøe, “Fault detection and isolation in centrifugal pumps,” *Department of Control Engineering, Aalborg Universitet*, 2005.

[17] Verdo A/S, Last visited 17-09-2017, https://verdo.dk/da/vand/forsyningskunde-/om-verdo-vand,Om Verdo Vand.

[18] D. Chen, *Sustainable Water Technologies*. Green Chemistry and Chemical Engineering, CRC Press, 2016.

[19] *Water Transmission and Distribution*. Principles and practices of water supply operations series, American Water Works Association, 2011.

[20] T. N. Jensen, C. S. Kallesøe, and R. Wisniewski, "Adaptive reference control for pressure management in water networks," *European Control Conference(ECC)*, vol. 3, July 2015.

[21] E. Agency, *Epanet 2 Users Manual.* CreateSpace Independent Publishing Platform, 2016.

[22] W. Borutzky, *Bond Graph Methodology.* Springer London, 2010.

[23] N. Deo, *Graph Theory with Applications to Engineering and Computer Science.* Dover Publications, 2017.

[24] S. Krantz, *Handbook of Complex Variables.* Birkhäuser Boston, 2012.

[25] L. Johnson, *Geographic Information Systems in Water Resources Engineering.* CRC Press, 2016.

[26] Verdo A/S, *Ledningnetmodel for Verdo's forsyningsområde.* Verdo, 2010.

Rettelser

Todo list